Study on the molecular mechanisms for high-light acclimation in the green alga *Chlamydomonas reinhardtii*

Yari Kamrani, Yousef

Doctor of Philosophy

Department of Basic Biology
School of Life Science
SOKENDAI (The Graduate University for Advanced Studies)

National University
SOKENDAI
The Graduate University for Advanced Studies

Study on the molecular mechanisms for high-light acclimation in the green alga *Chlamydomonas reinhardtii*

Yari Kamrani, Yousef

Ph.D. Thesis

Supervisor: Prof. Jun Minagawa

Okazaki, Japan 2018

Contents

Articles closely related to the subject of the thesis

Yousef Yari Kamrani, Takuya Matsuo, Maria Mittag, Jun Minagawa; ROC75 is an Attenuator for the Circadian Clock that Controls LHCSR3 Expression, *Plant and Cell Physiology*, Volume 59, Issue 12, 1 December 2018, Pages 2602–2607, https://doi.org/10.1093/pcp/pcy179

List of figures

Chapter 6

Fig 31 Diagrammatic scheme of the effect of blue light on cytosolic calcium concentration through organellar diffusion

Abstract

Chlamydomonas reinhardtii is a ~10-µm, unicellular green alga which can be easily grown and uniformly exposed to different light intensities in the laboratory. Each *C. reinhardtii* cell contains a single chloroplast; the photosynthetic apparatus of this alga is very similar to plants which makes it ideal for studying responses to excess light. Strong light intensity leads to harmful overexcitation of the photosystems; in *C. reinhardtii*, LHCSR3 is required for a quick protective response, known as energy-dependent quenching (qE). However, regulation of *LHCSR3* expression remains to be investigated. Since the majority of photoacclimation analyses has been conducted under controlled laboratory conditions, physiological responses to natural environmental changes are not well clarified; in plants and microalgae, light-dark cycles are required to synchronize circadian clocks to multiple physiological responses. However, clock response to high light has been the subject of speculation. Previously, 105 circadian rhythm insertional mutants were isolated as *rhythm of chloroplast* (*roc*) mutants. Moreover, very recent research has shown blue light perceived by PHOT (phototropin photoreceptor) mediates the photoprotection of the photosynthetic machinery and regulation of LHCSR3 in *C. reinhardtii*. In fact, downstream of PHOT, this signal integrates with another regulatory signal from the chloroplast that carries information about the amount of absorbed light that is not used for CO_2 fixation. This signal relies on photosynthetic electron transfer via an as-yet-unknown mechanism, and further relies on photosynthetic electron flow, which ultimately affects accumulation of *LHCSR3* transcript. The aim of my research was to determine how these mechanisms are involved and coordinated in the regulation of *LHCSR3* gene under high-light acclimation in *C. reinhardtii*. As a first step I characterized 105 ROC series mutants by qE value under strong blue and red light and I report *ROC75*, a putative transcriptional factor as a key component of the central circadian clock, which showed a significantly higher qE value and LHCSR3 protein accumulation than the wild type when grown under red light. Further, *LHCSR3* mRNA in *roc75* mutant exhibited a circadian rhythm, with its basal expression level higher than in the wild-type. I therefore conclude that ROC75 acts as an attenuator for the circadian clock that controls *LHCSR3* expression with red light as a negative stimulus. For the second step, I investigated that calcium (Ca^{2+}) dependent mechanisms are more substantial to both PHOT-dependent and photosynthetic signaling pathways. However, we know very little about the nature of cytosolic calcium ($[Ca^{2+}]_{cyt}$) elevation in microalgae. Therefore, I introduced Ca^{2+} fluorescent

probes into *C. reinhardtii* to monitor $[Ca^{2+}]_{cyt}$ variations, using confocal microscopy. I found that PHOT was involved in $[Ca^{2+}]_{cyt}$ increases induced by blue light, as $[Ca^{2+}]_{cyt}$ increased after a few seconds of blue light exposure in wild-type cells but not in *phot* mutant. Furthermore, I observed an increase of cytosolic Inositol 1,4,5-trisphosphate (IP_3) induced by blue light in wild-type cells but not in *phot* mutant. I then hypothesized that PHOT activates G proteins to produce IP_3 which leads to the activation of the IP_3 receptor (IP_3R) and a subsequent raise in intracellular Ca^{2+} levels. To examine this, I used a specific IP_3R blocker, Xestospongin C (XeC), which demonstrated that blue light can increase cytosolic Ca^{2+} level and this elevation is inhibited strongly in the presence of 5 µM XeC. Moreover, I specified that photosynthesis signals modulate $[Ca^{2+}]_{cyt}$ level since 5 µM DCMU (specific and sensitive inhibitor of photosynthesis) inhibited the increase in $[Ca^{2+}]_{cyt}$ levels of wild-type cells pre-treated for 1h with blue light and exposed to an acute stimulation with blue light (30 µmol photons $m^{-2}s^{-1}$). Based on these results and to reveal more important key players involved in the Ca^{2+} signaling dependent regulation of *LHCSR3*, a high throughput forward genetic approach was used to screen mutants using bioluminescence derived from a luciferase reporter gene fused to a full-length sequence of *LHCSR3* gene. 15 mutants have been isolated, identified and will be useful for future students.

In summary, my findings regarding the involvement of a circadian component into the photoprotection mechanisms provides a new viewpoint for thinking about the adaptive significance of the circadian clock. Herein I present the first evidence of involvement of circadian components into photoprotection in *C. reinhardtii*. For the second project, my finding implies that cytosolic Ca^{2+} is important factor for the integrated signal between PHOT and photosynthesis pathways and shed more light on the regulatory strategies behind photoprotection mechanism.

Abbreviations

ATP	Adenosine Triphosphate.
Ca2+	Calcium.
ER	Endoplamic Reticulum.
ETR	Electron Transport Rate
GPCR	G Protein-Coupled Receptors.
IP3	Inositol triphosphate.
IP3R	Inositol 1,4,5-trisphosphate receptors.
ROS	Reactive Oxygen Species.
RYR	Ryanodine receptors.
SERCA	Sarco/Endoplasmic Reticulum Ca^{2+}-ATPase pump.
$[Ca^{2+}]_{cyt}$	Cytosolic free calcium
Chl	Chlorophyll
LHC	Light Harvesting Complex
LHCSR	Light Harvesting Complex Stress-Related protein
NPQ	Non-photochemical quenching of chlorophyll fluorescence
PC	Plastocyanin
PSI	Photosystem I
PSII	Photosystem II
WT	wild type
LD	light/dark cycle
LL	low light
SD	standard deviation, Σ
DCMU	(3-(3,4-dichlorophenyl)-1,1-dimethylurea) is a photosynthesis inhibitor
XeC	Xestospongin C
qE	energy dependent quenching
Fluo-3	a fluorescence indicator of intracellular calcium (Ca^{2+})
PHOT	phototropin photoreceptor
pCRY	plant like cryptochrome
aCRY	animal-like cryptochrome

ROC	RHYTHM OF CHLOROPLAST
BL	blue light
Rd	red light
DD	constant dark
D	dark
UVB	ultraviolet B
CBB cycle	Calvin– Benson–Bassham

Chapter 1

Introduction

1.1. *Chlamydomonas* as a model

C. reinhardtii is a good model organism for studying responses to excess light due to it being easily grown in liquid or on agar in a wide range of environmental conditions. Because of this we can use a uniform population of *C. reinhardtii* cells to study changes in biochemistry and gene expression. Vascular plants are less useful for these types of studies due to having leaves that are made up of various types of tissue, and due to having layers that have different photoacclimation responses (Nishio, J.N., Sun, J. and Vogelmann, n.d.). *C. reinhardtii* makes it possible for us to gather large amounts of homogeneous experimental material because it is easy to grow and can be exposed to different light intensities in an even manner. The cells of *C. reinhardtii* have a single chloroplast and have photosynthetic machinery that is very much like that of vascular plants. However, photosynthesis is not required for *C. reinhardtii* to survive which makes it easy to isolate and analyze mutants that are light sensitive because of photoprotection defects (Erickson et al., 2015). *Chlamydomonas reinhardtii* is a ∼10-μm green alga with two anterior flagella, multiple mitochondria, and a chloroplast containing the cellular machinery for photosynthesis and metabolic pathways (Merchant et al., 2010). *Chlamydomonas*, in contrast to flowering plants, can be grown in the dark on an organic carbon source without losing its photosynthetic apparatus. which is why it is used to study eukaryotic photosynthesis. It is also a good model organism for studying the effect of defects in flagella and basal body functions (Keller et al., 2005). *Chlamydomonas* is also being used to research food color additives, bioremediation, and biofuel generation. Taken together this shows the value of *Chlamydomonas* as both a model organism and as a natural resource.

1.1.1. The origins of *Chlamydomonas* genes

Green algae, including *Chlamydomonas* and *Ostreococcus* (Chlorophytes), diverged from the land plants and their close relatives (Streptophytes) over a billion years ago. These are both part of the green plant lineage (Viridiplantae), which diverged from animals, fungi, and Choanozoa (opisthokonts) (Yoon et al., 2004). *Chlamydomonas* has many genes that can be shown to have diverged from the common ancestor of plants and animals by comparative genomic analyses.

The proteins found in *Chlamydomonas* are more similar to *Arabidopsis thaliana* than to human proteins in most cases. However, some *Chlamydomonas* proteins, such as those related to flagella, are quite similar to human orthologs. Most likely most of the genes necessary for forming and regulating flagella and basal bodies are lost in organisms that have evolved away these organelles (Cole, 2003).

2489 protein families of orthologs and paralogs of *Chlamydomonas* proteins were homologous to proteins from both *Arabidopsis* and humans. 706 protein families are shared with humans but not with *Arabidopsis*, indicating they were either lost or diverged beyond recognition in green plants. 1879 protein families are found in *Chlamydomonas* and *Arabidopsis* but have no human homologs (Merchant et al., 2010).

C. reinhardtii has been used to study many biological phenomena, which has given us an abundance of information about not only *Chlamydomonas*, but also about plants and animals (Harris, 2001).

1.2. Overview of photoprotection

Light can be harmful to photosynthetic organisms despite the fact that it is required for their growth in most cases. A wide range of fluctuating light conditions can be found in natural environments, from near total darkness to very high intensities at noontime, and these conditions can change rapidly over the course of a few seconds, or over longer diurnal and seasonal time scales. In low light conditions, the rate light is absorbed is well matched with the rate of photosynthesis (Erickson et al., 2015), which helps maximize photosynthetic efficiency (Björkman and Demmig, 1987). The photosynthetic machinery can become saturated as light increases in intensity, but this can lead to the absorption of more light than is necessary for the maximum photosynthetic rate (P_{max}) (Erickson et al., 2015). Because of this *C. reinhardtii* has acquired several ways to lessen light stress to defend against and repair damage caused by an overabundance of light. Light level changes, including short-term stress events (such as quick fluctuations in light intensity on partially cloudy days) and long-term stress events (such as being in direct sunlight for many hours per day) can be sensed and responded to by *C. reinhardtii*. Repair mechanisms mediate PSII turnover to

maintain photosynthetic capacity in *C. reinhardtii* when it is exposed to excess light over long periods. In addition, gene expressions occur to help acclimate the cell to high light conditions. If this over-excitation is not dealt with properly biologically damaging chemical intermediates and byproducts can be produced that cause photo-oxidative damage to the photosynthetic reaction centers. In aerobic environments reactive oxygen species (ROS) are the most common reactive byproducts of photosynthesis under high light stress (Niyogi, 1999) .

1.2.1. Dissipation of excess light

Photoprotective mechanisms exist for quenching excess ^{1}Chl* and dissipating the energy harmlessly as heat when light intensity is higher than the tolerance of the photosynthetic machinery. Chl* with asterisks shows short-lived singlet excited state of chlorophyll (Erickson et al., 2015). These mechanisms are measured from the reduction of Chl fluorescence from PSII and are referred to as non-photochemical quenching (NPQ) (Horton et al., 1996). NPQ consists of responses that occur over longer periods allowing for acclimation to high light exposure, as well as short-term responses to rapid fluctuations in light. There are four types of NPQ categorized based on the time scales of their induction and relaxation: energy-dependent feedback de-excitation quenching (qE) (Muller, 2001), zeaxanthin-dependent quenching (qZ) (Nilkens et al., 2010), state transition-dependent quenching (qT) (Minagawa, 2011), and photoinhibitory quenching (qI). which occurs during sustained dissipation of excitation energy as heat that continues over several hours. It has been attributed to photoinhibition of PSII (Somersalo and Krause, 1989).

1.2.2. Energy dependent NPQ (qE)

The most rapid type of NPQ is qE. As described above quick fluctuations in light intensity and quality requires mechanisms to dissipate excess absorbed light energy rapidly to avoid high light shock. qE can be induced in seconds and protects the photosynthetic machinery by reducing the lifetime of ^{1}Chl* in PSII, which consequently decreases O_2 generation (Aro et al., 1993) and by preventing damage to the oxygen-evolving complex caused by acidification of the thylakoid

lumen. Formation of a proton gradient (ΔpH) across the thylakoid membrane and a stress-related LHC protein, known as LHCSR (Peers et al., 2009) is required for qE induction.

Under high light conditions the pH of the luminal side of the thylakoid membrane is reduced due to overactive photosynthetic electron transport (Muller, 2001). The importance of ΔpH for qE can be seen with the addition of nigericin, an ionophore that inhibits ΔpH formation (Niyogi et al., 1997).

1.2.3. LHCSR3 is required for qE in algae and mosses

Isolation and characterization of *npq* mutants has identified two types of LHC proteins of *C. reinhardtii* that play roles in qE. The *npq4* mutation was mapped to an insertion that disrupts the expression of the stress-related LHC genes *LHCSR3.1* and *LHCSR3.2*, which encode identical LHCSR3 proteins (Peers et al., 2009). These two genes are regulated by nearly identical promoter regions and have nearly identical DNA sequences (Maruyama et al., 2014). The *LHCSR1* gene encodes another isoform of LHCSR, which is found upstream of *LHCSR3.1* and *LHCSR3.2* on the same chromosome. All three *LHCSR* genes are transcriptionally up-regulated in response to high light.

1.2.4. Regulation of *LHCSR3* transcription

1.2.4.1. Photosynthetic electron transfer

Maruyama et al., found that accumulation of *LHCSR3* transcripts were highly induced when cells kept in low light conditions were exposed to 1 h of high light. However, they also found that DCMU (at 10 μM) inhibited LHCSR3 expression in wild-type cells exposed to high light for 1 h (Maruyama et al., 2014). DCMU blocks photosynthetic electron transfer at the Qb site of PSII.

1.2.4.2. CO2 concentration

Yamano et al. (Yamano et al., 2008) showed that the transcription of *LHCSR3* (*Li818r-1*) was induced under a low-to-high light transition, but these genes responded to fluctuations in CO_2 concentration quite differently. This is consistent with the presence of the EEC element in the *LHCSR3.1* locus, but not in *LHCSR1*.

1.2.4.3. Blue light dependent regulation of LHCSR3 by phototropin

Previously our lab reported that Blue light was more effective than red light in inducing the qE response and LHCSR3 accumulation, although the cells absorbed both almost equally. Moreover, animal-like cryptochrome mutant cells (deficient in a functional aCRY gene, hereafter acry) showed wild-type levels of qE and LHCSR3 accumulation. On the other hand, phototropin mutant cells (deficient in a functional PHOT gene, hereafter phot) were more prone to photodamage due to lacking blue-light induction of qE and LHCSR3 accumulation. It was therefore concluded blue light perceived by PHOT mediates the photoprotection of the photosynthetic machinery (qE) in a green alga (Petroutsos et al., 2016). However downstream signaling of phot to regulate LHCSR3 expression remains to be investigated.

1.2.4.4. The necessity of calcium signaling in LHCSR3 induction

Petroutsos et al. (Petroutsos et al., 2011) reported that experiments with a calmodulin antagonist, *N*-(6-aminohexyl)-5-chloro-1-naphthelene-sulfonamid-hydrochloride (W7), at a concentration of 25 μM W7 showed a clear decrease in induction of LHCSR3. As a negative control W5 (biologicaly inactive analog W5 [*N*-(6-aminohexyl)-1-naphthelene-sulfonamid-hydrochloride) did not show an impact, even at concentrations as high as 100 μM.

1.2.5. CAS protein regulates LHCSR3 expression

It has been reported that CAS (a thylakoid Ca^{2+}-binding protein) mediates the transient elevation of cytosolic Ca^{2+} concentration ($[Ca^{2+}]_{cyt}$), as well as stromal Ca^{2+} concentration ($[Ca^{2+}]_{stro}$), in guard cells of *A. thaliana* and regulates plant immune responses. In *Chlamydomonas*, an ortholog of CAS (Cre12.g497300) was also detected in the thylakoid membrane fraction. It has been suggested that CAS is required not only for photoacclimation by regulating induction of LHCSR3 but is also required, under anaerobic conditions, for making a super complex for photosynthetic cyclic electron flow (CEF) and has a possible role in the CO2 concentrating mechanism. While the molecular mechanisms are not yet totally clarified, the impact of Ca^{2+} and CAS on qE indicates

a connection between acidification of the thylakoid lumen and regulation of CEF by Ca^{2+} (Petroutsos et al., 2011).

To understand the possible role of Ca^{2+} signaling in photoacclimation, I further reviewed the literature focused on Ca^{2+} signaling in land plants and *Chlamydomonas reinhardtii*.

1.3. Calcium-dependent regulation of photosynthesis

Plant cells react to diverse developmental conditions and environmental factors by increasing cytoplasmic calcium $[Ca^{2+}]_{cyt}$. Alterations in $[Ca^{2+}]_{cyt}$ are reported to be vital for physiological responses in plants. Over 30 separate developmental processes and environmental factors initiate changes in the $[Ca^{2+}]_{cyt}$ (White and Broadley, 2003). There is evidence that chloroplasts contribute to cytosolic Ca^{2+} signaling through CAS. Although the details of this mechanism have not been resolved, cytosolic Ca^{2+} signals could not be generated in CAS knock out mutants through application of external Ca^{2+} (Weinl et al., 2008). It has been suggested that modifications in chloroplast Ca^{2+} concentration affect enzymatic functions of Ca^{2+}-binding proteins in the chloroplast and regulate the oxygen evolving capacity of PSII and the NPQ mechanism (Hochmal et al., 2015).

1.3.1. Ca^{2+} dynamics in plant chloroplasts

Chloroplasts possess a high concentration of Ca^{2+}. A large part of chloroplastic Ca^{2+} (~15 mM) (Portis and Heldt, 1976) is bound to the negatively charged thylakoid membranes or to calcium-binding proteins. This keeps the resting free $[Ca^{2+}]$stroma as low as 150 nM. It has been shown that light-dependent uptake of Ca^{2+} occurs in isolated chloroplasts. However, the molecular mechanisms regulating this process are yet to be clarified.

1.3.2. Phototropin-dependent calcium mobilization in *A. thaliana*

Baum et al. used de-etiolated whole seedlings of *A. thaliana*. that had been transformed with cytosol- or organelle-targeted aequorin, a luminescent protein that is calcium-sensitive, to elucidate the phot1-dependent elevation of cytosolic Ca^{2+} (Baum et al., 1999; Harada and Shimazaki, 2007). Ten seconds of blue-light irradiation is sufficient to induce a transient increase in cytosolic Ca^{2+}, but not in the chloroplasts and nucleus. In cry1 and cry2 mutants the blue light-dependent increase of Ca^{2+} was not observed. The phot1 (nph1) mutant however exhibited only half of the increase compared to the wild type, this implies that the Ca^{2+} increase was partly mediated by phot1.

1.3.3. Relationships between blue light-dependent responses and calcium

Baum et al. further demonstrated that pretreatment of tobacco seedlings with red light had a strong inhibitory effect on blue light-dependent increase in cytosolic Ca^{2+} (Baum et al., 1999). Moreover, U-73122 blocks phospholipase C (PLC) activity and therefore reduces the amount of inositol 1,4,5-triphosphate (previously InsP3, now IP_3), as a result activation of Ca^{2+} release from internal stores such as ER or vacuoles is inhibited. In their model phot2 is suggested to induce PLC activity as shown in Fig 1 (Harada and Shimazaki, 2007).

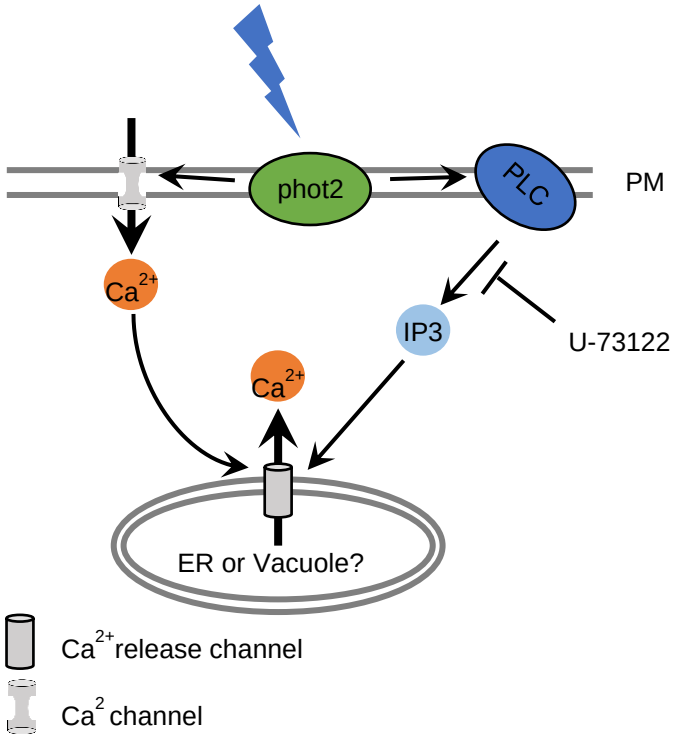

Fig 1 A schematic model of the signal pathway of phot1- and phot2-dependent increase in $[Ca^{2+}]_{cyt}$ in leaves of *A. thaliana*. Modified from Harada et al 2003.

Vascular plants do not have clear homologues of some important Ca^{2+} channels found in animals, such as the four domain voltage-dependent Ca^{2+} channels (VDCCs), the transient receptor potential (TRP) channels and the inositol triphosphate receptor (IP3R) (Edel and Kudla, 2015; Wheeler and Brownlee, 2008). However, these channels are present in green algal genomes (Merchant et al., 2010; Wheeler and Brownlee, 2008), suggesting that there may be important differences in the signaling mechanisms between plants and green algae. While $[Ca^{2+}]_{cyt}$ elevations in plants have been extensively characterized (McAinsh and Pittman, 2009), direct observations of $[Ca^{2+}]_{cyt}$ elevations in green algae remain limited.

IP3R subunits are encoded by three genes in vertebrates. IP3R subunits form large-conductance Ca^{2+}-permeable channels within intracellular membranes, especially those of the ER. Opening of the central pore is initiated by binding of IP_3 to the specific IP_3 binding site of IP_3R, which make conformational changes within the N-terminal domains of IP3R (Fig 2). These conformational changes consequently facilitate binding of Ca^{2+}, which then triggers opening of the channel. Thus,

IP3R activation requires both cytosolicIP3 and Ca^{2+}. Subsequent studies confirmed that PKA stimulates phosphorylation of hepatic IP3Rs and potentiates IP3-evoked Ca^{2+} release. In separate studies it has been shown that cyclic AMP also modulates this pathway by, for example, regulating PLC and the coupling of receptors to PLC (Taylor and Tovey, 2010).

Therefore, at least two routes through which cAMP can directly modulate IP3R gating exist. Phosphorylation of IP3R by PKA increases the efficiency of IP3 and Ca^{2+} activation of channel opening.

It is worth noting Xestospongin C, extracted from the sponge *Xestospongia sp*., is a well-known membrane-permeable inhibitor of the IP3-mediated Ca^{2+} release (Gafni et al., 1997).

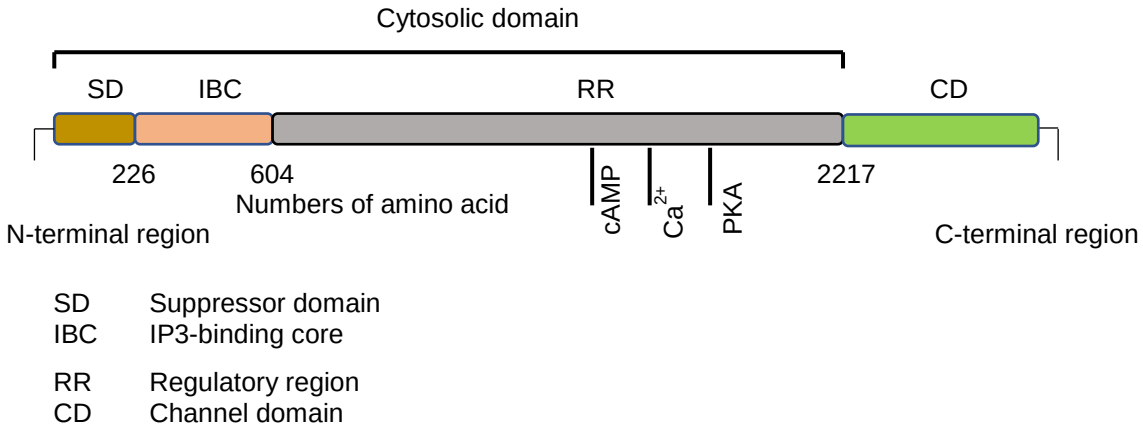

Fig 2 Domain organization of global architecture of IP_3R. Full name of each domain appears below the graphic.

1.4. Challenges

As PHOT regulate LHCSR3 expression in *C. reinhardtii* and Ca^{2+} is required for the accumulation of LHCSR3, a relationship between PHOT, Ca^{2+}, and LHCSR3 is likely. It was proposed that other second messengers, such as the cyclic nucleotides cAMP or cGMP, act as the signalling molecules downstream of PHOT. Using a pharmacological approach, this hypothesis was tested and found that treatment of *phot* cells with 3-isobutyl-1-methylxanthine (IBMX), an inhibitor of cAMP and cGMP phosphodiesterases which results in accumulation of intracellular cAMP and activation of PKA (protein kinase A) , rescued LHCSR3 expression (Petroutsos et al., 2016). Indeed IBMX is a competitive nonselective phosphodiesterase inhibitor of PDE, which raise cAMP accumulation in cytosol (Weiss and Hait, 1977). This effect was confirmed by incubating *phot* cells with dibutyrylated cGMP and cAMP (DB-cGMP and DB-cAMP, suggesting that cyclic nucleotides are not only critical in mating and phototaxis, but are also involved in photoprotection in *C. reinhardtii* through the regulation of LHCSR3 expression.

While the role of Ca^{2+} signalling in flagellar-related processes in *C. reinhardtii* is well established (Collingridge et al., 2012; Quarmby et al., 1992; Quarmby and Hartzell, 1994), its role in regulating processes in the cell body has been less thoroughly explored. Recent progress indicates a role for Ca^{2+} in the cellular responses to nutrient starvation (Motiwalla et al., 2014) and in regulating photoacclimation, through the activity of the chloroplast-localized calcium sensor protein (CAS) (Petroutsos et al., 2011). However, the dynamics of $[Ca^{2+}]_{cyt}$ elevations in response to these and other environmental stimuli in *C. reinhardtii* have not been characterized.
Therefore, all this evidence led to the hypothesis that cytosolic Ca^{2+} might be the key factor in elucidating:

1. Downstream signaling of PHOT to regulate LHCSR3
2. Downstream signaling of photosynthetic electron transfer (ETR) to regulate LHCSR3
3. And finally, the intermediate signaling between ETR and PHOT signaling pathways to regulate LHCSR3 gene expression.

In order to gain a better understanding of the role of Ca^{2+} signalling in green algae, we performed a detailed examination of the dynamics of $[Ca^{2+}]_{cyt}$ elevations generated by *C. reinhardtii* cells in response to blue light.

1.5. Aims

In this dissertation, I investigate the molecular mechanisms behind regulation of *LHCSR3* in *Chlamydomonas reinhardtii*. As described above the LHCSR3 protein plays a crucial role in the qE mechanism to dissipate excessive light. Specifically, I have the following aims:

1. Investigate the impact of the circadian clock on regulation of *LHCSR3*. Due to the versatile function of ROC series mutants in *Chlamydomonas* we focus mainly on characterization of these clock mutants with respect to qE value and LHCSR3 expression under strong blue and red light. This model is discussed in section 3.1.

2. Establish and develop techniques to visualize cytosolic Ca^{2+} in *Chlamydomonas* and use this approach to investigate those molecular mechanisms which are involved downstream of phototropin and ETR to regulate *LHCSR3* expression. These results are discussed in section 3.2.

3. Exploring our achievement in calcium signaling for designing a high throughput forward genetic screening using random insertional mutagenesis to pinpoint more important factors and elements involved in blue-light-calcium signaling-dependent regulation of *LHCSR3* gene. The result of this part is discussed in 3.3.

Chapter 2

Materials and Methods

2.1. Materials

2.1.1. Primers

Table 1: List of primers I used for all three projects.

Primer ID/analyze	Sequence	Target
Fw.P .Jajek1/insertion check	ACACGTACAGGAGCGCAAC	IP_3R
Rv.P.Jajek1/insertion check	CAGGAGTCCTTGTCCAACCAG	IP_3R
LETM1-NdeI-Fw/cDNA cloning	TTTTCATATGATGCGGTCGTCACTTCCAACGAG	CPLD62
LETM-KpnI-Rv/cDNA cloning	TTTTGGTACCCGCTTGCTTGCGGCTTG	CPLD62
LET-FW1/partial cDNA cloning	GTCCTCCACGAAGAAGCAGG	CPLD62
LET-RV1/partial cDNA cloning	CTTGAGCTGCTCCGCCAC	CPLD62
LET-FW2/partial cDNA cloning	GCCGGGTTGCGCTCGCTG	CPLD62
LET-RV2/partial cDNA cloning	CTGCAGGACCGCGTGCAG	CPLD62
LET-FW3/partial cDNA cloning	GTGGCCATCCAGCTCAAGG	CPLD62
LET-RV3/partial cDNA cloning	CTAACCATGATCTCCTGGCGG	CPLD62
LET-FW4/partial cDNA cloning	GTATGAGGAGCTGGAGCGGC	CPLD62
LET-RV4/partial cDNA cloning	CTTCTGTGTCGCCTCCTGCAG	CPLD62
CaM11-Fw/ insertion check	ACCTCGTTGCTGCACGTC	CAM11
CaM11-RV/insertion	TGGCGATATGCAGCCTTGC	CAM11
ROC59-FW/qPCR	AGTCTGGGCTGCACCAGC	ROC59
ROC59-RV/qPCR	ATGGCGCCGGTGATCACG	ROC59
ROC75-FW/qPCR	AGGACAAGAACGGAGAACG	ROC75
ROC75-RV/qPCR	TGTAATAGCCGGGCTTCTC	ROC75
LHCSR3.1-FW/qPCR	CACAACACCTTGATGCGAGATG	LHCSR3.1
LHCSR3.1-RV/qPCR	CCGTGTCTTGTCAGTCCCTG	LHCSR3.1
LHCSR3.2-FW/qPCR	TGTGAGGCACTCTGGTGAAG	LHCSR3.2
LHCSR3.2-RV/qPCR	CGCCTGTTGTCACCATCTTA	LHCSR3.2
CBLP-FW/qPCR	CAAGTACACCATTGGCGAGC	CBLP
CBLP-RV/qPCR	CTTGCAGTTGGTCAGGTTCC	CBLP

DegPstI/RESDA PCR	CCAGTGAGCAGAGTGACGIIIIINNSCTGCAGW	random
Deg SacII/RESDA PCR	CCAGTGAGCAGAGTGACGIIIIINNSCCGCGGW	random
Deg BglII/RESDA PCR	CCAGTGAGCAGAGTGACGIIIIINNSAGATCTS	random
Deg MluI/RESDA PCR	CCAGTGAGCAGAGTGACGIIIIINNSACGCGTW	random
Q0/RESDA PCR	CCAGTGAGCAGAGTGACG	5′ end of deg primers
aph7tag-R1/RESDA PCR	AGCGGCTGCAAATGGAAACG	DNA marker
aph7tag-R2/RESDA PCR	GATGCTGCTTGAGACAGCGAC	DNA marker
aph7tag-R3/RESDA PCR	CTCCCAGAATTCCTGGTCGTTC	DNA marker
aph7tag-F1/RESDA PCR	GACGTCTATGCGGGAGACTC	DNA marker
aph7tag-F2/RESDA PCR	CTTCGAGGTGTTCGAGGAGACC	DNA marker
aph7tag-F3	GTAAATGGAGGCGCTCGTTGATC	DNA marker
LHCSR3.1-P-F1	TCTCGAATTCGCTGACTCCCCTGTCTTCAG	LHCSR3.1 promoter
LHCSR3.1-P-R1	TCGCTTTAAATGTGAGTGCAAGTGGCGTGCA	LHCSR3.1 promoter
pRT-LHCSR3-seq1	GAGGCCATGAAGCGCTACGG	pRT-LHCSR3-LUC plasmid
pRT-LHCSR3-seq2	CGCCATCCTGAGCGTGGTGCC	pRT-LHCSR3-LUC plasmid
pRT-LHCSR3-seq3	GAAATGGACCGCGCTCATCA	pRT-LHCSR3-LUC plasmid

2.1.2. Plasmids

pRT-GenD-CrmVenus_aphVIII

pHSG/lucNCi-TRBCS2

pCR 2.1 TOPO/luc tag

pRT-GenD-LHCSR3.1 (+Cla)_aphVIII

pRT-GenD-LHCSR3.1(+Cla)-lucNCi _aphVIII

p3xHA-2xgp64-3xFLAG-Letm1

2.1.3. Kits

Table 2: List of commercial kits I used for all three projects

Kit name	Purpose
QIAprep spin Miniprep kit-QIAGEN	DNA miniprep
PCR clean-up Gel extraction-Macherey Nagel GmbH&Co-Germany	PCR product and agarose gel-based DNA purification
ReverTra Ace® qPCR RT Master Mix with gDNA Remover-TOYOBO Co,LTD	cDNA synthesis
RNeasy® Mini Kit (250)-QIAGEN	RNA extraction
DIG High Prime DNA Labelling and Detection Starter Kit II	Southern blot

2.1.4. Lab equipment

Table 3: Commonly used equipment for my study in Minagawa lab

Machine	Purpose
NANODROP 2000c Thermo scientific	Measuring DNA/RNA concentration, OD_{730nm}
ChemiiDoc XRS+ Imaging system-BIO-RAD	Image DNA, Western Blot
LightCycler 96 Roche	qPCR analysis
FlourCam 800MF Photon Systems Instrument	Images of chlorophyll fluorescence signal
CHURITSU	Bioluminescence assay
Fr light ISC-201-2 CCS	Power Supply for LED Small Lighting in far red
Voertex2Genie2	Variable speed control shaking or vortexing

Pipetman and Nichipet EX PlusII	Mechanical single channel pipettes
16ºC incubator ETB ThermpoBucket	Non-water insulation incubator used for ligation procedure
Mupid-eXu electrophoresis system	Standard type of *electrophoresis system* with agarose gel
SimpliAmp Thermal cycle-applied Biosystems	thermal cycler for PCR workflow
Micro-Mixer E-36 TAITEC	Shaker of 96 well plates and microtubes. Switchable speed between high and low
Personal-10 TAITEC 37ºC incubator	37ºC incubator for *E.coli* broth culture
TOMY MX-205 microcentrifuge	High speed refrigerated micro centrifuge
SANYO Biomedical freezer	Freezer used for -20, -30 and -80 º C storage
LED INSIGHT Valore	LEDs 400,470,550,660,730nm
TOSHIBA	fluorescent lamp peak at 450nm
AIRTECH cleanbench	laminar flow *clean bench equipped with UVC lamps*
New Brunsweek scientific Excella E5 platform shaker	100-300 ml flask shaker for *Chlamydomonas* cells growth
$NEPA21_{TypeII}$ NEPAGENE	Electroporator
TOMY LSX-500	970mm autoclave
himac CT 6E Hitachi	15 or 50 ml falcon tube centrifuge, max speed 2500 rpm
Attune acoustic focusing cytometer applied biosystems	flow cytometry used for Cell counting and viability/bleaching

2.1.5. Media and solutions

TAP medium

Tris base	2.42 g
Tap salt	25 ml
Hutner trace elements	1 ml
1 M KPO4 (pH 7.0)	1 ml
pH 7.0 by Acetic acid	1.05 ml
water to 1 liter	

phosphate solution

K_2HPO_4	288.0 g
KH_2PO_4	144.0 g
water to 1 liter	

high salt medium

MOPS	4.19 g
Beijernick's solution	5 ml
Hutner trace elements	1 ml
1 M KPO4 (pH 7.0)	13.5 ml
pH 7.0 by 10 M KOH	~ 0.95
water to 1 liter	

Beijerinck's solution

NH_4Cl	100.0 g
$MgSO_4 . 7H_2O$	4.0 g
$CaCl_2 . 2H_2O$	2.0 g
water to 1 liter	

Hutner trace elements

EDTA disodium salt	50 g	250 ml
$ZnSO_4 . 7 H_2O$	22 g	100 ml
H_3BO_3	11.4 g	200 ml
$MnCl_2 . 4 H_2O$	5.06 g	50 ml
$CoCl_2. 6 H_2O$	1.61 g	50 ml
$CuSO_4 . 5 H_2O$	1.57 g	50 ml
$(NH_4)_6Mo_7O_{24}. 4 H_2O$	1.10 g	50 ml
$FeSO_4. 7 H_2O$	4.99 g	50 ml

2.2. Methods

2.2.1. Strains and conditions.

Two *Chlamydomonas reinhardtii* wild-type strains SAG73.72 (mt+) (Müller et al., 2017) and CBR34 (Matsuo et al., 2008), were grown in flasks with orbital shaking (~125 rpm) under 15 μ mol photons m−2 s−1 white light (Fluorescent Lamp, Toshiba) in Tris-acetate-phosphate (TAP) media (Gorman and Levine, 1965) at 23 °C and switched to high-salt (HS) media (Sueoka, 1960) at 3 million cells ml−1 and irradiated with different light intensities as described in the text and figure legends. The *roc* series mutants were gifted from Dr. Takuya Matsuo, Nagoya university. The *pcry* (Müller et al., 2017) and *phot* (Zorin et al., 2009) mutants were used for quantitative PCR analysis. For continuous-dark treatments, flasks doubly wrapped with aluminum foil were

used to culture aliquots. For LD cycle experiment of Figure 7, *Chlamydomonas* wild type and *pcry* mutant cells were entrained under 12 h light:dark cycles for three days. The 12 h light period was designed in three section (3:6:3 h red:red+green+blue:red respectively) to imitate natural light at morning, noon and early evening. LEDs were used for light treatment were including blue (450nm), green (550nm) and red (660nm), with 100 μmol m-2s-1 equally of each LED lights. Cells were collected for RNA extraction and qPCR analysis after exposed 1h to 250 μmol photons $m^{-2} \cdot s^{-1}$ of blue light at the end of the 12 h of dark period of the LD regime.

2.2.2. Immunoblot analysis

Western blot analysis was performed as described previously (Takahashi et al., 2006). The whole cell protein extracts were loaded on 12% SDS–PAGE gels and blotted onto nitrocellulose membranes. We used Rabbit monoclonal anti-LHCSR3 antibody (1:1,000; Agriseraas) as the primary antibody. For the secondary antibody horseradish peroxidase (HRP) conjugated antibodies were used. ATPB was used as a loading control.

2.2.3. Photosynthetic measurements

For measurement of qE induction, cells were first treated for 12 minutes with far-red light to fully achieve maximum chlorophyll fluorescence (Fm), which was measured with a 600-ms saturating pulse. The actinic light intensity was 900 μmol photons $m^{-2} \cdot s^{-1}$. qE was calculated as (Fm − Fm')/Fm', where Fm' is the maximum yield of fluorescence in the presence of actinic light. Before qE measurements, cells were exposed to high-intensity light for 4 h. For action spectrum measurements, cells (4×10^6 cells ml^{-1}) were placed in a 12-well plate and exposed to intense (250 μmol photons $m^{-2} \cdot s^{-1}$) monochromatic light-emitting diode light (the spectral half width is ±12 nm-NK system, Japan) for 4 hours. Samples were collected for either immunoblotting or qE measurement (Fluorcam 800MF, Photon System Instruments)

2.2.4. Loading with fluorescent dyes

For loading with Fluo3-AM dye (Thermofisher scientific- F1242), I used Braun and Hegemann 1999 method with modification briefly, *Chlamydomonas* cells exposed to dark or blue light (30 mE) for 1h at room temperature and were centrifuged for 3 min at 2200 rpm, washed twice and

resuspended to a cell density of 2 x 10^6 cells/ml in 1 mL of NMDG+/K+ buffer (5 mM HEPES, 10 mM HC1, 1 mM KC1, 200 µM K^+-BAPTA, pH= 5.6), containing 1 mM sulfinpyrazone (dissolved by increasing temporarily pH of buffer to ~9). pH was adjusted with Nmethyl-D-glucamine (NMG- SIGMA: CAS Number 6284-40-8) and CaCI2). Suspension of *Chlamydomonas* seeded on glass coverslips (pre-coated with poly-L-lysine for at least 20 minutes). *Poly-L-Lysine* (PLL) is a synthetic molecules used to enhance cell attachment to *glass* surfaces. 2 µL of Fluo3-AM added to the suspension (final concentration = 10 µM) followed by incubation of cells for 2 h at 37˚C, in the dark and finally cells rinsed in NMDG+/K+ (calcium free) and fluorescence emitted at 520 nm (acquisition with 40X lens) was recorded.

All imaging was performed using an Olympus Confocal Laser Scanning Microscope FV3000 with 40x objective. The following excitation and emission settings were used: Venus, 514 excitation with 543/22 emission; Fluo3-AM, 488 excitation with 525 emission; and chlorophyll, 561 excitation with 685/40 emission. All confocal microscopy images were analyzed using ImageJ. In parallel with every single experiment, we imaged C137 wild type cells without any probe and with the same exact microscopy settings to see how much autofluorescence signal for normalization.

2.2.5. Transformation and genetic crosses

Nuclear genome transformation of *Chlamydomonas* C13 wild type cells was performed using electroporator NEPA21 (Nepa Gene company-Japan) according to manufacture protocol (Shimogawara et al., 1998). Briefly, cells were harvested in late exponential phase (count cells by hemocytometer confirming the density 1~ 2.5 x 10^6 cells/mL) and resuspended in TAP at concentration of 1 x 10^8 cells per mL. Afterwards, 300ng DNA (linearized by *KpnI* for pHSG-LhCSR3.1p-Luci-AphVIII and DraI for p3xHA-2xgp64-3xFLAG-Letm1 digestion) and 0.05 mL of 40 mM sucrose were added to 0.1 mL cell suspension. The cell suspension of 0.15 –mL was placed into a disposable electroporation cuvette with a 2-mm gap (NEPA., Japan). Multiple decaying pulses using the model NEPA21 type II (NEPAGENE, Japan) electroporation apparatus.

Table 4: The set up of electroporation process used for transformation by NEPA21

	Poring Pulse						Transfer Pulse					
Program channel #	Voltage (V)	Pulse length (ms)	Pulse interval (ms)	# of pulse	Polarity	Decay rate (%)	Voltage (V)	Pulse length (ms)	Pulse interval (ms)	# of pulse	Polarity	Decay Rate (%)
11	250	5	50	2	+	10	8	50	50	±5	+/-	40
13	300	3	50	2	+	10	8	50	50	±5	+/-	40
14	300	5	50	2	+	10	8	50	50	±5	+/-	40

Poring pulse around 300 volts open the hole in the plasma and nuclear membrane and a transfer pulse which is longer with low voltage transport negatively charged nucleic acid molecules into cells and nuclei. Decaying pulses elevate the efficiency without further suffering the cells. Transformants transferred into a fresh 8-mL TAP. Cell suspension was incubated under light (40 µmols photons m^{-2} s^{-1}, white) overnight. Cells were collected by centrifugation (2500 rpm for 5min R.T) and plated on TAP agar medium containing 10 µg / mL paromomycin or 20 µg / mL spectinomycin. Plated cells incubated in 24°C at 100 µmols photons m^{-2} s^{-1}, white light for three days. Fig 3 shows a photographic image of hygromycin resistant colonies grown after 8 days of plating.

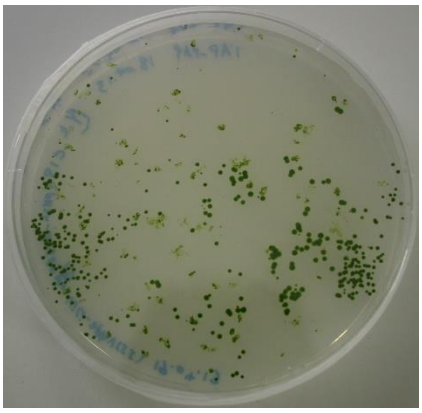

Fig 3 Colonies of paromomycin-resistant transformants plated on TAP agar medium containing 10 μg mL^{-1} paromomycin. Its important tiny colonies also be chosen since mutant phenotype may cause defect in growth.

Well grown either paromomycin or spectinomycin resistant colonies were picked up and inoculated in 96 multiwell plates filled up with 200 μl TAP medium for growing four days in room temperature (24°C) at 40 μmols photons m^{-2} s^{-1}, white light.

2.2.6. Genetic cross-cosegregation analysis

Mt^+ and mt^- cells were mixed in 96-well plates in nitrogen-free TAP medium for 2 days under 50 μmols photons m^{-2} s^{-1} white light. In fact, nitrogen limitation is the initiating signal for mating and gametogenesis. Cells were washed several times with fresh TAP-N to remove unmated cells. After about five days the mature zygospores adhered to the walls and bottoms of the wells were observed. Then, the plates were incubated about 2 hours in -20 ºC to fully eliminate residual unmated cells, and zygotes were germinated by adding complete TAP medium. After further 3 days under same light condition as above, zygotes were hatched, and progenies spread on TAP agar plates, and those colonies could grow on the plates were subjected to random progeny analyses. For cosegregation analysis, the colonies were cultured in 96-well plates for 3 d, and 5-μL of the cultures were inoculated in HS medium in 96-well plates for the bioluminescence assay and the same clone on TAP agar plates containing 10 μg/mL hygromycin B (Sigma) for the hygromycin resistance test (Fig 4). Pairs with the same mating type strain served as negative controls to confirm complete elimination of unmated cells.

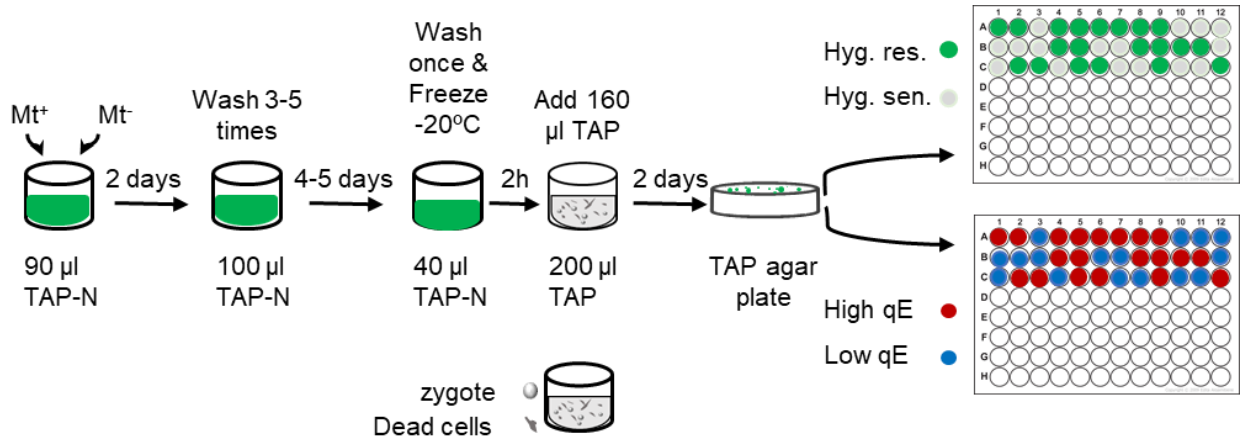

Fig 4 Graphic illustration of the cosegregation analysis to determine whether hygromycin res. cassette is responsible for mutant phenotype

Bioluminescence assay

100 µl of high light or dark treated cells were transferred to a white 96-well plate and luciferin potassium salt (Biosynth, Staad, Switzerland) was added and mixed at a final concentration of 100 µM. Bioluminescence assay was performed after incubating the mixture in dark for 210 seconds.

2.2.7. RESDA PCR

The restriction enzyme site-directed amplification PCR (RESDA-PCR) technique was developed originally by González-Ballester et al. (González-Ballester et al., 2005)which is based on degenerated primers that anneal with sequences of restriction sites highly and randomly distributed along the genome, and its specificity is ensured by a nested PCR. More common restriction site sequences are designed to be at the 3′ end with a few numbers of degenerations to raise the chances of the primer binding. These sequences are joined to another specific sequence at their 5′ end by a bridge of inosines. Four restriction sites *Pst*I, *Sac*II, *BglII* and *Mlul* were selected for the degenerated primers. An 18 bp adapter sequence was added to increase specificity of amplified bands, which raise the probability one of these four restriction sites be close enough to the insertion which in turn leads to amplification of a specific product. Lists of primers are described below:

Primers

Degenerated primers

DegPstI : CCAGTGAGCAGAGTGACGIIIIINNSCTGCAGW

Deg SacII : CCAGTGAGCAGAGTGACGIIIIINNSCCGCGGW

Deg BglII : CCAGTGAGCAGAGTGACGIIIIINNSAGATCTS

Deg MluI : CCAGTGAGCAGAGTGACGIIIIINNSACGCGTW

Q0 : CCAGTGAGCAGAGTGACG

aph7-tag specific primers

<u>for promoter side</u>

aph7tag-R1, aph7tag-R2, aph7tag-R3

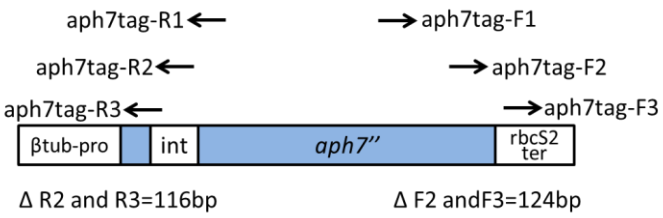

<u>for terminator side</u>

aph7tag-F1 , aph7tag-F2, aph7tag-F3

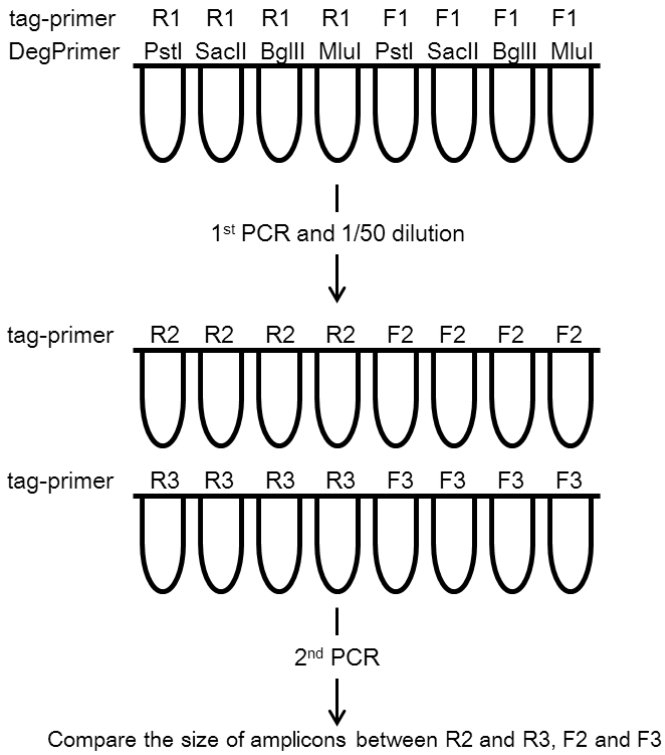

2.2.8. Construction of the *LHCSR3.1-pLUC* reporter gene

aphVIII as a selection marker was amplified from pRT-GenD-CrmVenus_aphVIII vector as template by PCR with the primer sets aphVIII-F1 (5′- gcctctttctccatgctcgagcggggagctcgctg-3′)/ aphVIII-R1 (5′- attacgccaagcttgggtacccgcttcaaatacgcc-3′) and inserted into linearized pHSG/lucNCi-TRBCS2 vector (*NcoI, sphI*) gifted form Dr. Takuya Matsuo-Nagoya university. LHCSR3.1 promoter was amplified from genomic DNA by PCR with the primer sets *LHCSR3.1*-P-F1(FW:5'-TCTCGAATTCGCTGACTCCCCTGTCTTCAG-3')/*LHCSR3.1*-P-R1(5'-TCGCTTTAAATGTGAGTGCAAGTGGCGTGCAA-3') 1500bp upstream of ATG start codon to cover promoter region.

To construct *LHCSR3.1* translational fusion, luciferase gene from pCR 2.1 TOPO/luc tag vector was cut using ClaI and this fragment ligated to linearized pRT-GenD-LHCSR3.1 (+Cla)_aphVIII with ClaI restriction enzyme. LHCSR3.1 in this plasmid was entire gene fragment including exons and introns. Plasmid were digested afterwards to verify the presence of the insert (luciferase) and for determining its orientation in the entry vector. Restriction digestion reaction was done with

ScaI. Three Primers were used for sequencing of final construct harboring pRT-GenD-LHCSR3.1(+Cla)-lucNCi _aphVIII . pRT-LHCSR3-seq1 (5'-GAGGCCATGAAGCGCTACGG-3')/ pRT-LHCSR3-seq2 (5' CGCCATCCTGAGCGTGGTGCC-3')/ and pRT-LHCSR3-seq3 (5'-GAAATGGACCGCGCTCATCA -3')

2.2.9. RNA analyses

Total RNA was extracted by using TRIzol/chloroform reagent following the manufacturer's instructions QIAGEN RNeasy kit (Life Technologies Japan, Tokyo, Japan). Briefly, cells were disrupted with glass beads in TRIzol Reagent and, passed through one-time chloroform extraction, and total RNA was extracted from the aqueous phase using RNeasy Mini kit. After quantification of total RNA amount using nanodrop, reverse transcription and quantitative real-time PCR was done using a ReverTra Ace cDNA synthesis kit (Toyobo). qRT-PCR was performed with KOD SYBR qPCR Mix (Toyobo) with LightCycler 96 (Roche). The primers listed in Table 1 were used for RT-PCR and qRT-PCR. All data sets were analyzed using ABI Prism SDS software (Applied Biosystems).

2.2.10. Preparation of genomic DNA

To prepare genomic DNA, cells were grown in TAP medium, harvested in stationary phase by centrifugation, and suspended in 1/5 volume of TEN wash buffer and pellets were suspended in in 1/10 SDS-EB /proteinase K after centrifugation. A series of subsequent centrifugation followed by suspension cells in PCI, CI and aqueous phase was transferred to a new tube with 0.1ml high salt TE/RNase A and mixture was incubate at 37˚C for one hour. Final step was EtOH precipitation followed by 70% EtOH wash and resuspension of dried pellet in nuclease free H_20.

2.2.11. Calmodulin Inhibitors

Calmodulin (CaM) and calmodulin KII (CaMKII) inhibitors W7 and KN-93 respectively were purchased from TCI (Tokyo chemical industry co.). W7 was prepared as a 5 M stock in ethanol. KN-93 were prepared as 1.0 mM stocks in water and were used at a final concentration of 5.0 μM (Sumi et al., 1991). Inhibitors added to HS medium under low light 10 minutes prior to high light incubation.

2.2.12. Phylogenetic tree construction

The LETM-like gene sequences were conceptually translated into proteins and used for multiple sequence alignment and phylogenetic analysis as described previously (Maruyama et al., 2011). IQ-TREE was used to reconstruct phylogenetic trees using LG + F + I + G4 model (Nguyen et al., 2015). The model used for tree (in this case, LG + F + I + G4) is dependent on the dataset.

2.2.13. IP-1 assay

Measurement of IP-1 concentration was based on Cisbio company's kit and HTRF® technology. This bioassay kit measures IP1 accumulation levels in cells. In a standard state, the interaction between the donor and the acceptor produces a fluorescent signal. Briefly, low light adopted cells treated with LiCl (25-50mM) to accumulate IPOne in presence of either 30 minutes low light (20 $\mu mol \cdot m^{-2} s^{-1}$ white light) or 30 min blue light (100 $\mu mol \cdot m^{-2} s^{-1}$ 450nm). 200000 cells/tube were pelleted. Pelleted cells incubated 30 minutes at 37ºC and the experiment followed by adding anti IP-1 cryptate and IP-1-d2 and incubated 1 hour at room temperature according to Cisbio IP-one assay kit protocol. The signal is expressed in DeltaF in % (DF%) which is a comparative standard curve (DF%).

$$DF\% = \frac{Ratio_{pos.control} - Ratio_{neg.control}}{Ratio_{neg.control}} \times 100$$

2.2.14 TMHMM program

TMHMM approach is applied for prediction of transmembrane protein. TMHMM is based on a hidden Markov model. Recent reports showed that it can correctly predict 97-98% of the transmembrane helices. Moreover, TMHMM can distinguish with high accuracy between membrane and soluble proteins (Krogh et al., 2001).

2.2.15. Complementation of the mutant phenotype by *Letm1* gene

The plasmid carrying the LETM1 full cDNA (NdeI/KpnI fragment - 2709bp), was constructed and cloned along with the bacterial *aadA* gene which codes for streptomycin resistance as a reliable selectable marker **(**Goldschmidt-Clermont, M. 1991) into p3xHA-2xgp64-3xFLAG(C) gifted kindly from Dr. Tomohito Yamasaki and is available in *Chlamydomonas* Resource Center (www.chlamycollection.org/). Letm1 cDNA is GC rich (some region exceeds 81% GC) that results in cloning unusual difficulties, this challenge already has been reported among many *Chlamydomonas* genes; therefore, cloning passed through a series of short fragment PCR amplification followed by second PCR and third PCR reactions using first and second PCR product respectively as templates to fully amplify cDNA region. At the end, sequencing analysis confirmed the constructed plasmid didn't have any point mutation, deletion or changes and linearized at DraI site before transformation into *letm1* mutant strain for complementation analysis. I am in this step of analysis now and I will soon proceed with transformation of complemented construct and screening.

2.2.16. LETM1 anti-transport Ca^{2+} and H^{+} in vitro

To investigate activity and confirm whether LETM1 forms a functional transporter I first cloned *Letm1* cDNA as described above and this fragment is in process to be expressed in *Escherichia coli* system and the purified recombinant protein will be analyzed through the cation including Ca^{2+} flux monitoring in presence of pH gradient by using patch clamp method. The patch-clamp technique allows the investigation of even single ion channel opening event.

Chapter 3

ROC75 is an Attenuator for the Circadian that Controls LHCSR3 Expression

3.1. Summary of work

In green algae, strong light intensity leads to harmful overexcitation of the photosystems. In *Chlamydomonas reinhardtii*, LHCSR3 is required for a quick protective response, known as qE quenching. However, regulation of *LHCSR3* expression is yet to be fully understood. Since the majority of photoacclimation analysis has been conducted under controlled laboratory conditions, physiological responses to natural environmental changes such as light/dark cycles have not been examined in detail. In higher plants and microalgae, light-dark cycles are required to synchronize circadian clocks to multiple physiological responses for fitness. However, in photosynthetic organisms, clock response to high light has been the subject of speculation. Previously, 105 circadian rhythm insertional mutants were isolated as *rhythm of chloroplast* (*roc*) mutants. In this study, we report characterization of the *roc75* mutant, which showed a significantly higher qE value as well as LHCSR3 protein accumulation than the WT when grown under red light. Because the effect of ROC75 was red-light dependent, LHCSR3 expression might be mediated by a yet unknown red light photoreceptor. The effect of ROC75 was not dependent upon blue light although LHCSR3 was previously demonstrated to be under the control of blue light photoreceptor, phototropin. We performed transcript analysis of *ROC75* in the *pcry* (plant-cryptochrome) and *phot* mutants and found that only the former mutant accumulated a higher amount of *ROC75* mRNA, which suggests PCRY negatively regulates ROC75. Furthermore, the *LHCSR3* mRNA in the *roc75* mutant exhibited a circadian rhythm, but its basal expression level was higher than in the WT. We therefore conclude that ROC75 acts as an attenuator for the circadian clock that controls *LHCSR3* expression with blue and red light as a positive and a negative stimulus, respectively.

3.2. Brief Introduction

As the majority of photoacclimation analysis has been conducted under controlled laboratory conditions, physiological responses to natural environmental changes, such as light/dark (LD) cycles, have not been clarified in detail. These environmental time cues, termed *Zeitgebers* (German for ‘time givers’), train the endogenous timing system to synchronize to a period of 24 hours, precisely corresponding to the exogenous period of the Earth’s rotation (Ehlers et al., 1988;

McClung, 2006). From the perspective of fitness, light-dark or temperature cycles are required to entrain circadian clocks in higher plants and microalgae for multiple physiological responses (Stangherlin and Reddy, 2013). Nevertheless, in photosynthetic organisms, clock responses to high-light (HL) stress remain under debate (Sanchez et al., 2011).

In a previous study, 105 circadian rhythm insertional mutants were isolated as *rhythm of chloroplast* (*roc*) mutants. Characterization of these *roc* mutants has revealed a plethora of processes covering such diverse cellular processes as ubiquitin–proteasome interactions, transcription and transcript metabolism, gene silencing, membrane trafficking and transport, signal transduction, and DNA damage response (Matsuo et al., 2008).

In the present study, we investigated the possible role of circadian ROC proteins on photoacclimation, particularly LHCSR3 regulation under conditions of HL stress. Our findings regarding the involvement of a circadian component in photoprotection mechanisms provide a new viewpoint for the adaptive importance of the circadian clock. Herein, we present the first evidence of the involvement of circadian components in photoprotection in *C. reinhardtii*.

3.3. Results

3.3.1. qE based choice of 105 ROC series mutant under strong red light

We examined the mutant phenotypes for qE (pH- or energy dependent quenching) ability and Fv/Fm (maximum quantum efficiency of photosystem II) to determine if mutants show different levels of photosensitivity. Fv/Fm primarily reflects reduction in PSII activity and qE is the major and most rapid component of non-photochemical quenching (NPQ). Briefly, the low light adopted wild-type and *roc* series mutant cells irradiated for 5 hours with 250 µmol·m−2·s−1 of either blue (450nm) or red (660nm) light in high salt media after which qE capacity and Fv/Fm were measured as described in method. Two mutants with very high and low qE respectively, *roc75* and *roc59,* were chosen for further characterization. Since this phenotypic shift was significantly more pronounced under strong red light conditions, we highlighted them in two-dimensional plots of qE versus Fv/Fm in *roc* series mutants and CBR wild type cells, as shown in Fig 5. Under these growth conditions, the *roc75* mutant, a potential suppressor of qE was concluded to be less prone to

photodamage by showing higher Fv/Fm. The relative increase of maximum quantum efficiency in the mutant appears to be largely indicative of higher induction of the qE response. However, neither mutant exhibited any major differences in photosynthetic parameters when grown in LL. In previous research, *roc75* exhibited low-amplitude phenotypes in both the chloroplast bioluminescence and growth rhythms compared to wild type cells in low light adapted conditions(Matsuo et al., 2008). As previous reports (Matsuo et al., 2008; Matsuo and Ishiura, 2011; Niwa et al., 2013) have elucidated the importance of ROC75 as a key component of the central circadian clock, in this study we predominantly focused on characterization of this mutant.

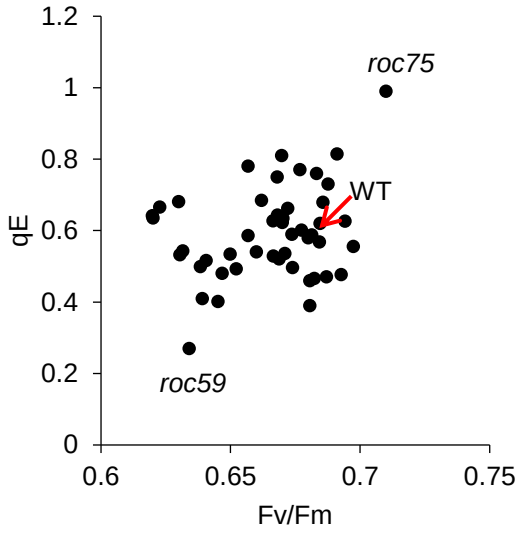

Fig 5 Photosynthetic characteristics of ROC series mutants under strong red light. CBR34^{+} WT and roc series mutant cells were exposed to 250 μmol·m^{-2}·s^{-1} red light (660nm) for 5 hours. The quantum yield of PSII (Fv/Fm) X axis values were determined by chlorophyll fluorescence measurements of dark adapted cells. Afterwards, qE values were measured with cells incubated 5 minutes with 750 μmol·m^{-2}·s^{-1} actinic light in the presence or absence of 10 μM nigericin.

3.3.2. *roc75* mutant exhibited high wavelength phenotypic shifts

Since photoreceptors play a critical role in both training the circadian clock and LHCSR3 regulation (Millar, 2003; Müller et al., 2017; Petroutsos et al., 2016) , to attain further insight into how ROC75 regulates LHCSR3 expression and qE induction under varying light quality, we measured the action spectrum of roc75 and compared with wild type cells (Fig. 6A). The action spectrum of qE induction for roc75 when exposed to 5h of 250 μmol·m−2·s−1 monochromatic

light showed very high in the red light region but was unaffected in the blue region. We analyzed LHCSR3 protein accumulation in *roc75* mutant cells using the same experimental conditions in Fig 5A. Through this we determined LHCSR3 accumulation in the red region is nearly as high as that for blue light (Fig 6B). This would indicate that there are at least two different pathways in *C. reinhardtii* that allow it to sense and respond to different colors of light. Because the effect of *roc75* was red light dependent, LHCSR3 expression might be mediated by an as yet unknown red light photoreceptor. On the other hand, no altered LHCSR3 level in blue light shows that either ROC75 is insensitive to blue light, or that a blue light photoreceptor represses ROC75, resulting in a neutral effect on LHCSR3 regulation. Two complementation lines of *roc75* cells with the full-length *ROC75* cDNA was able to fully rescue qE and LHCSR3 levels after 5h of treatment with 250µmol·m−2·s−1 red light supporting that it was functional (Fig 6 C, D)

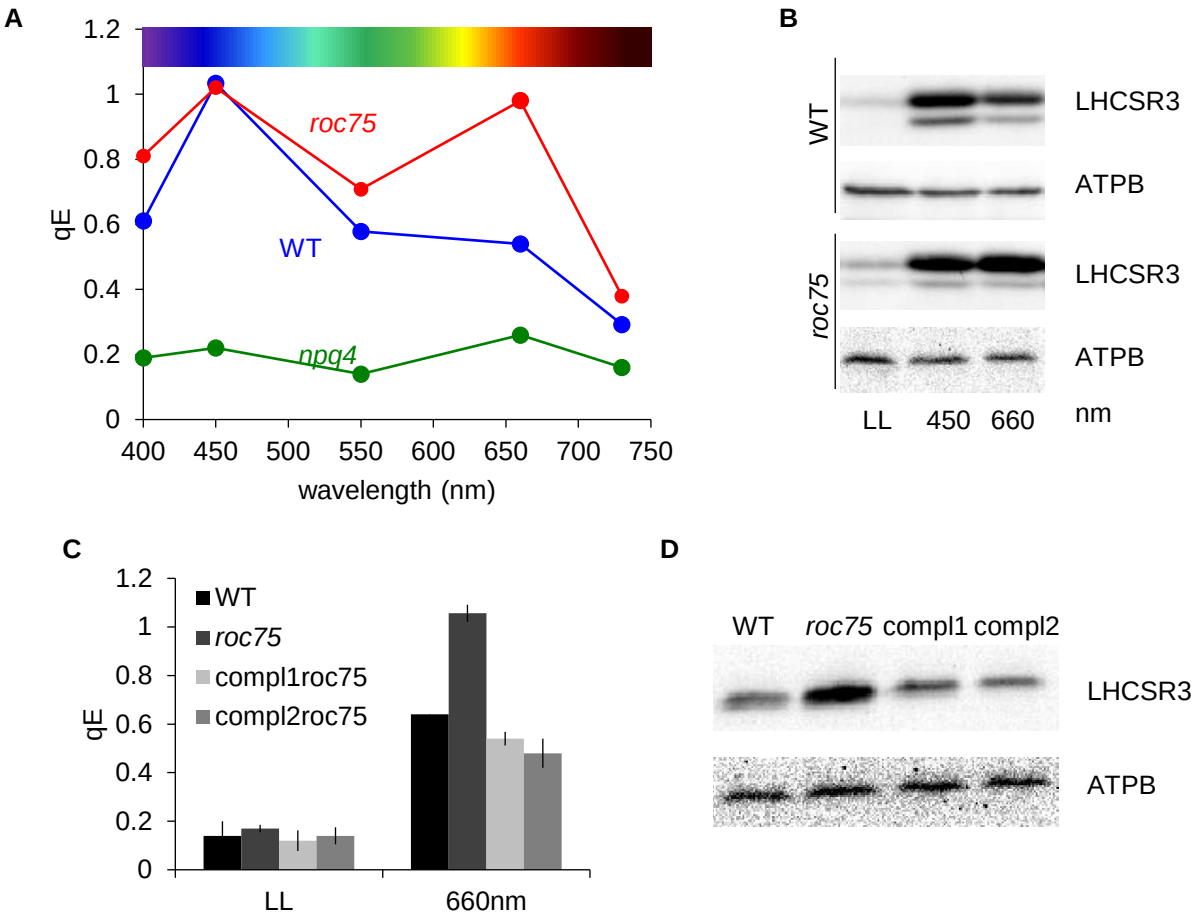

Fig 6 qE measurements and immunoblot analysis of LHCSR3 protein under various monochromatic lights. (A) qE induction in wild-type (WT; blue), *roc75* (red) and *npq4* mutant (green) under 5 hour illumination with the different wavelengths of light (250 μmol photons m−2 s−1). *n*=3 biological samples, mean±1Σ (B) immunoblot analysis of LHCSR3 accumulation under LL (low light: 20 μ mol photons m−2 s−1 white light) blue and red light with same experimental condition as A (ATPB is the loading control). (C) qE value of wild-type, *roc75* and two complemented line of *roc75* after 5-h exposure to 250 μmol photons m−2 s−1 red light, (D) immunoblot analysis of LHCSR3 accumulation with the same experimental conditions as (C).

3.3.3. pCRY attenuates *ROC75* expression under blue light

The effect of *roc75* was not dependent upon blue light (Fig. 6A and B), even though LHCSR3 was previously demonstrated to be under the control of the blue light photoreceptor PHOT (Petroutsos et al., 2016). We thus performed transcript analysis of *ROC75* in the *pcry* (plant-cryptochrome) and *phot* mutants which were entrained to a light–dark (LD) cycle for 3 days (see Methods for details). We found that only the former mutant accumulated a lower level of *ROC75* mRNA after blue light exposure in comparison to WT cells, which suggests that pCRY positively regulates *ROC75* (Fig. 7A and B). On the other hand, previous studies showed that pCRY accumulates under dark conditions and is degraded upon exposure to light (Reisdorph and Small, 2004; Müller et al., 2017). Therefore, by 2 h after dawn (Müller et al., 2017), degradation of pCRY leads to attenuation of *ROC75* expression. In fact, the degradation of pCRY contributes to prevent over accumulation of ROC75, which in turn facilitates the PHOT mediated main activation pathway for LHCSR3.

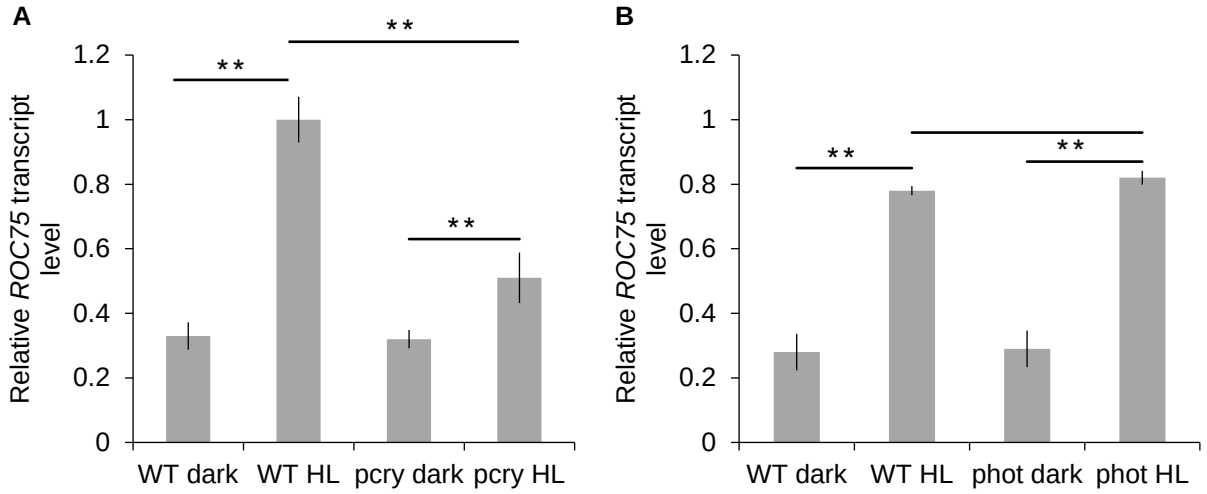

Fig 7 Real-time PCR analysis of the *roc75* transcript levels in two blue light receptor cell lines. (A) *ROC75* transcript accumulation in WT and *pcry* cells was measured using qRT-PCR after 2-h red light exposure (250 μmol photons m−2 s−1). (B) *ROC75* transcript accumulation in WT and *phot* cells with same experimental conditions as A. CT values of samples were normalized against CT values of GBLP as a housekeeping gene. (*n* = 3 biological samples; error bars represent SD).

3.3.4. The basal expression level of LHCSR3 is under the control of ROC75

The circadian rhythm in mRNA level of *LHCSR3.1*, *LHCSR3.2* of *roc75* mutant and wild type was examined (shown in Fig 8). The experimental condition were HS medium cultures of WT and *roc75* mutant which were entrained to LD cycle as described in the methodology. Both *LHCSR3* genes showed robust circadian rhythms peaking at early subjective day, while they were suppressed during the late subjective day into the subjective night.

Our results exhibited strong induction of *LHCSR3* in *roc75* mostly likely due to loss of the circadian clock mediated suppression mechanisms in this mutant for the LHCSR genes. Therefore, based on this analysis we conclude that the basal expression level of LHCSR3 is under the circadian control and furthermore, the repression of *LHCSR3* from the late subjective day to the late subjective night (i.e., 32-44 hr, 56-68hr) is attenuated by the mutation of ROC75. However, we conclude that this repression is not a direct repression by ROC75, since ROC75 is suggested to be a day phase expressed gene (Niwa et al., 2013). For a circadian biology researcher, knowledge of adaptive significances of the clock is of great interest, as it is generally believed that

circadian clocks have evolved to confer adaptive significances on organisms (Sharma, 2003; Yerushalmi and Green, 2009).

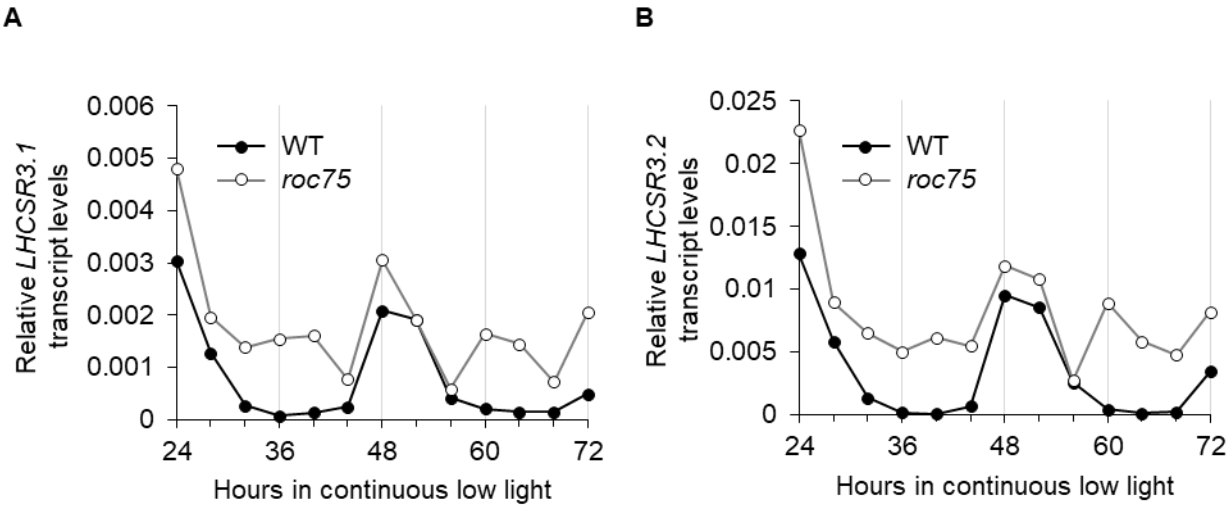

Fig. 8 Analysis of *LHCSR3* expression in LD under *roc75* mutant. Transcripts of both isoforms of *LHCSR3* named *LHCSR3.1* and *LHCSR3.2* were measured using qRT-PCR in WT and *roc75* mutant which were entrained to LD cycle and released into a continuous white light.

3.3.5. *roc59* shows lower accumulation of LHCSR3

Our preliminary data shows that under control of roc59, LHCSR3 accumulation as well as qE induction is much lower than wild type when cells were treated for 4 hours with 250 $\mu mol \cdot m^{-2} \cdot s^{-1}$ with red light suggesting ROC59 has a role as an activator of LHCSR3 likewise under control of ROC75 (Fig 9). However, more experiments are needed to clarify further circadian clock dependent regulation of LHCSR3 expression. Our findings, to our knowledge, are the first evidence of the involvement of circadian components into the photoprotection systems, further providing a new viewpoint for thinking about the adaptive significance of the circadian clock.

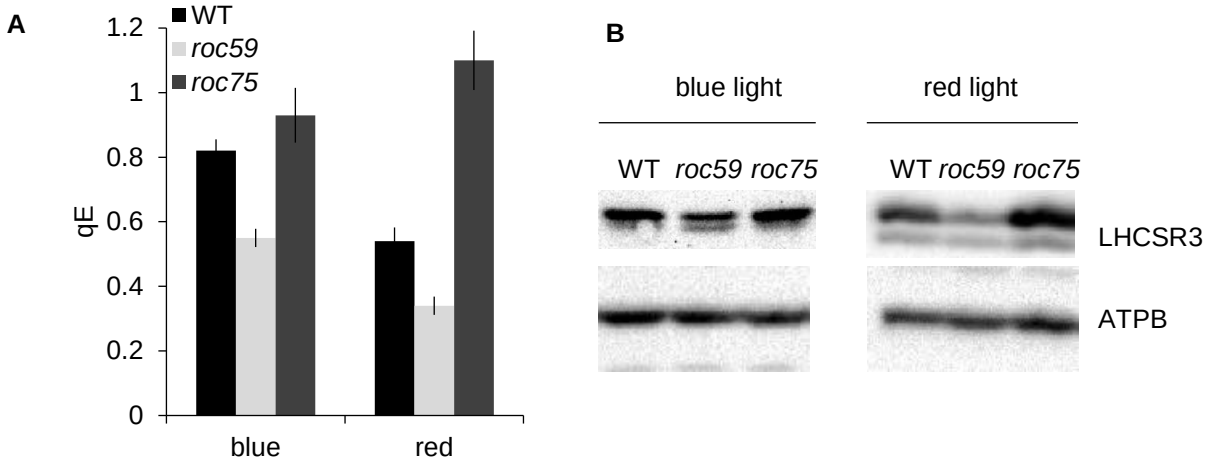

Fig 9 qE measurements and immunoblot analysis of LHCSR3 protein in WT, *roc59* and *roc75* mutants under strong blue and red light. Cells were grown under low white light and harvested after 5h illumination with 250 µmol photons m^{-2} s^{-1} blue (450nm) or red (660nm). (A) qE level of wild type and circadian mutant cells measured with strong actinic light (750 µmol m^{-2} s^{-1}) followed by dark NPQ relaxation. (B) Western blot analysis on LHCSR3 protein accumulation in acclimated cells. AtpB was used as loading control.

3.4. Discussion

Our results support the hypothesis that red light is an important component of the visible spectrum involved in the circadian clock signalling network in *C. reinhardtii* by controlling changes in qE induction and LHCSR3 expression (Fig 6).

If we clarify the impact of red light in natural environments, it may elucidate its important role and further reveal the necessity of the circadian clock as a controller of photoprotection, guaranteeing that photoacclimation mechanisms work properly. Basically, in morning and evening time, red light is the major component of visible light. These changes throughout the day, where towards noon time the ratio of blue light dramatically increases. It has been reported that strong blue light intensity causes photodamage to the oxygen evolving complex of photosystem II (Ohnishi et al.,

2005; Zavafer et al., 2015) therefore the accumulation of LHCSR3 for dissipation of excessive energy is essential during high blue light time periods. In the morning time the presence of LHCSR3 is not necessary since damage caused by blue light is less of a concern, so an unknown red light photoreceptor activates ROC75 to attenuate LHCSR3 expression. While as noon approaches, along with the damage potential of higher energy light, the increased blue light maintains degradation of the photoreceptor pCRY protein, which in turn results in attenuation of *ROC75* expression (Fig 7) to permit activation of LHCSR3 expression. This model is summarized graphically in Fig 10.

We have observed in an outdoor pond experiment, timelag for accumulation of LHCSR3. Where LHCSR3 induction initiates around 11:00 and drops slightly around 18:00 (data not shown, Dr. H. Yamasaki, personal communication) which supports our hypothesis. The contribution of circadian clock to this entire mechanism of photoacclimation helps microalgae to not only be synchronized with environmental changes, but also to determine the magnitude of different responses to better harness their resources, energy and feedback mechanisms, to ensure survival and improve the fitness of the individual.

We therefore conclude that ROC75 acts as an attenuator for the circadian clock that controls *LHCSR3* expression with blue and red light as a positive and a negative stimulus, respectively. On the other hand, since as described before, ROC75 is involved in the central mechanism of *Chlamydomonas* circadian clock control, combined with ROC75 being a DNA binding transcriptional factor, the involvement of other peripheral circadian oscillators downstream of ROC75 is not unexpected.

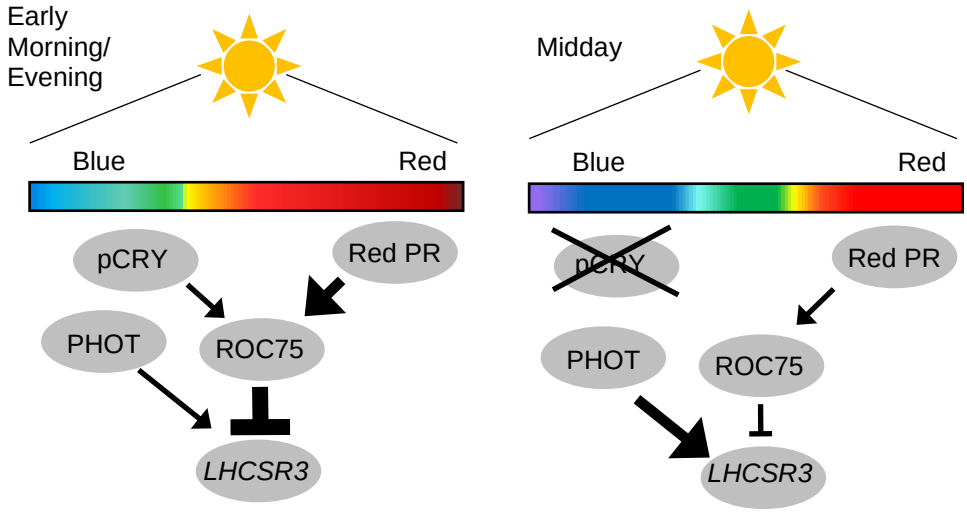

Fig 10 Schematic diagram of our proposed mechanism of roc75 control of *LHCSR3* expression. Three photoreceptors, PHOT, pCRY, and an unknown red photoreceptor, involved in the expression of LHCSR3 are depicted. Details are described in the text.

Chapter 4

Modulation of cytosolic Ca^{2+} has a key role in regulation of LHCSR3

4.1. Summary of work

To address those questions raised in introduction about the possible role of cytosolic calcium in regulation of LHCSR3 expression, in this section I used non-genetic encode calcium indicators for calcium imaging process to monitor cytosolic calcium elevation in addition with molecular and biochemical analysis. This project is still in process but to date I could determine blue light elicits phototropin-dependent cytosolic Ca^{2+} increase in *C.* reinhardtii. Moreover, cytosolic IP_3 concentration was under blue light dependent phototropin regulation. Since previous work in our lab clarified *LHCSR3.1* gene expression is under control of calmodulin using calmodulin specific inhibitor W7, I further analyzed whether calmodulin KII also is involved in this mechanism; by qPCR analysis of wild type cells treated with calmodulin K II selective inhibitor, I could confirm the involvement of Calmodulin KII. Furthermore, I could determine cAMP also as a second messenger regulates LHCSR3 expression via Phot-dependent Ca^{2+} signaling. However, although Xestospongin C (IP_3R specific blocker) exhibited very strong effect on repression of *LHCSR3.1* gene expression, *ip3r* knock out mutants in my experimental condition didn't show such strong effect. Further analysis is needed to confirm this result.

4.2. Brief introduction

As briefly described in introduction, both photosynthesis signal (ETR) and PHOT signal are needed for regulation of LHCSR3 expression as both pathways are mutually dependent on each other as simplified graphic below shows. Moreover, Dimitris et al. suggested that a second messenger such as Ca^{2+} could constitute the intermediate between these two signaling pathways (Fig 11).

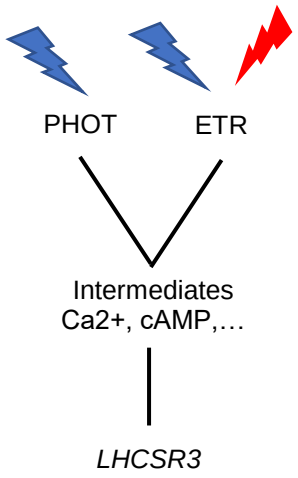

Fig 11 **A simplified illustration of two signaling pathways involve in regulation of *LHCSR3* gene expression.** Each individual pathway and possible intermediates described in introduction.

As with many plant cell types, the visualization of Ca^{2+} elevations in individual cells of the green algae has proved problematic, although the recent biolistic loading of dextran-conjugated dyes (Bothwell et al., 2006) has enabled the study of Ca^{2+} signaling during the process of flagellar excision (Wheeler and Brownlee, 2008).

Therefore, I applied a novel method to visualize cytosolic calcium signaling in *Chlamydomonas reinhardtii* using calcium indicator dyes, which are BAPTA-based organic molecules that change their spectral properties in response to the binding of Ca^{2+} ions.

My aim in this section was to use calcium imaging in order to respond to several questions, as pointed out below:

Since $[Ca^{2+}]_{cyt}$ signaling and in particular ER stress have not yet been investigated in *Chlamydomonas*, I hypothesized a model (as seen below in Fig 12) describing how LHCSR3 gene expression could be modulated via PHOT-dependent cytosolic Ca^{2+} signaling. This model is based

on the knowledge from plant and mammalian cytosolic calcium signaling and homology-based prediction of domain structures of the *Chlamydomonas* proteins.

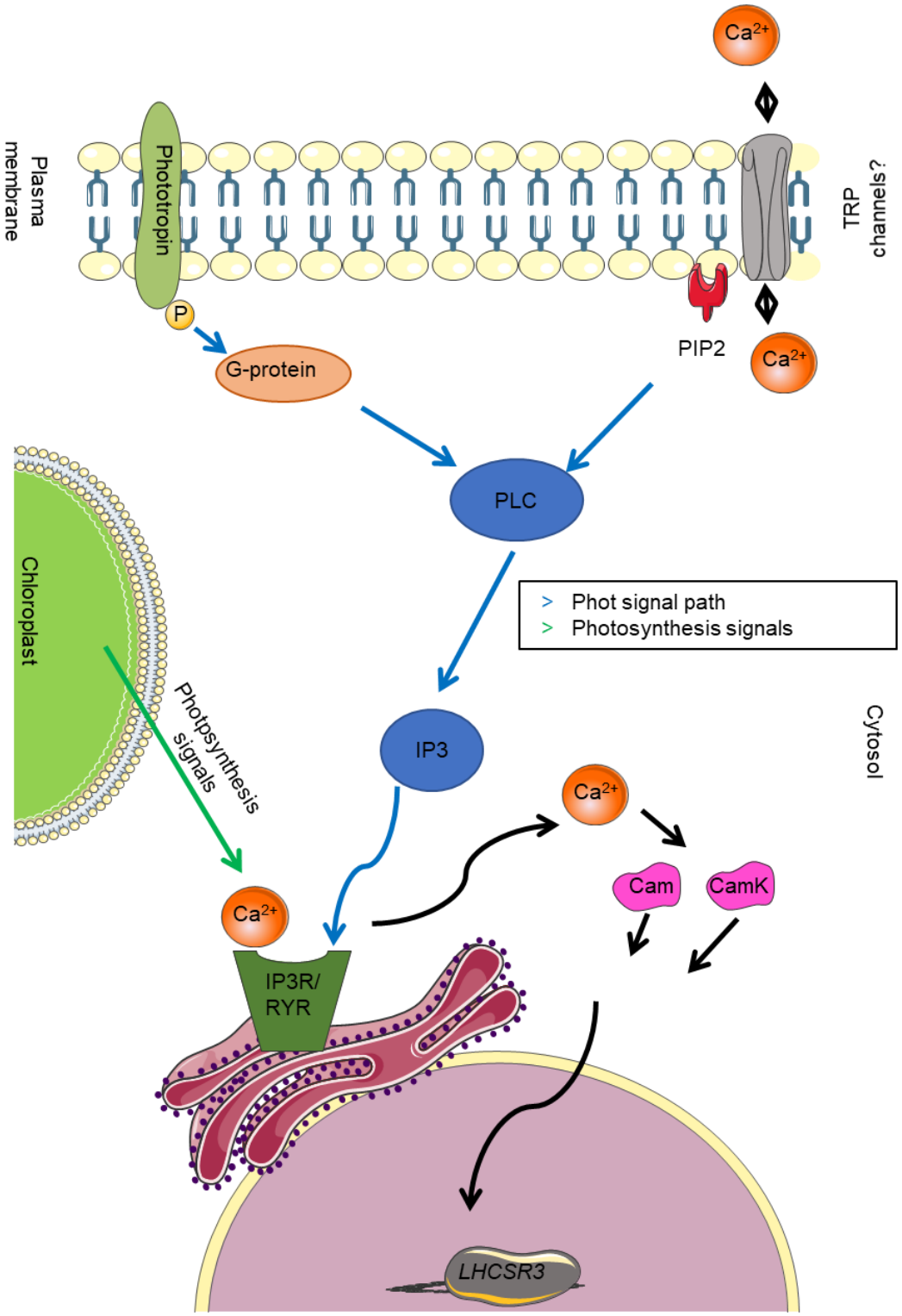

Fig 12 A minimal proposed model for the calcium signaling pathway by which phototropin regulates *LHCSR3.1* in *C. reinhardtii*. This model illustrates LHCSR3.1 gene expression is under regulation of $[Ca^{2+}]_{cyt}$ which is assumed to be released form ER. Calcium release from ER is under control of IP_3R protein which is localized across ER membrane. IP_3R function or regulation has not been investigated in *Chlamydpmonas reinhardtii* however in my hypothesis IP3 (generated by PHOT pathway) and Ca^{2+} (efflux from chloroplast triggered by high light) are needed to release high concentration of calcium from ER by binding to IP_3R.

4.3. Results

4.3.1. Blue light elicits phototropin-dependent cytosolic Ca^{2+} increase in *C. reinhardtii*

As described in the introduction, plant phototropin seems to be involved in the regulation of cytosolic Ca^{2+} levels. Here, we report for the first time that the basal level of cytosolic Ca^{2+} in *Chlamydomonas* can be increased by 1-hour illumination with blue light (30 $\mu mol \cdot m^{-2} \cdot s^{-1}$) in comparison with WT sample maintained in the dark, and this elevation was not observed in *phot* mutant (Fig 13 A). However, as observed in Fig 13 A, the Ca^{2+} basal level of samples maintained in the dark was not very low, possibly due to illumination of our cells during their growth. In parallel, I also investigated the effect of an acute exposure to blue light on *Chlamydomonas*. Fig 13 B shows the mean Ca^{2+} imaging traces of WT (black) and *phot* mutant (red) cells exposed to an acute stimulation with blue light (30 $\mu mol \cdot m^{-2} \cdot s^{-1}$) and recorded in extracellular Ca^{2+}-free condition. As we observe in this figure, free cytosolic Ca^{2+} increases almost instantaneously after blue light treatment in WT cells but not in *phot* mutant cells. This result suggested that blue light triggers a rapid Ca^{2+} signaling pathway involving release from intracellular stores, since the recordings were performed in the absence of extracellular Ca^{2+}.

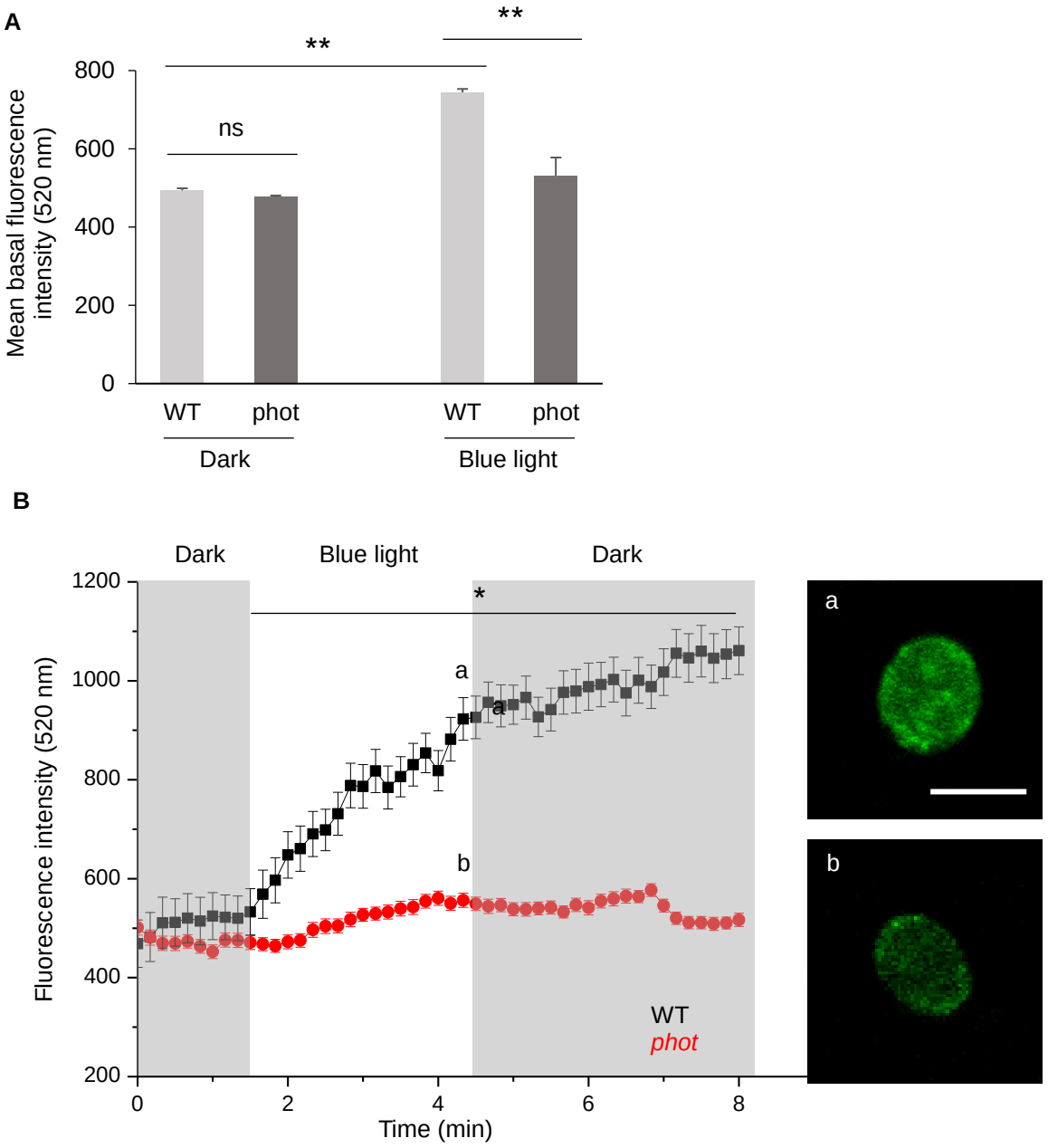

Fig 13 *Phot* mutant exhibit lower Ca^{2+} levels. (A) effect of phot on Basal cytosolic Ca^{2+} levels under blue light of WT, *phot* mutant recorded in calcium-free condition after an 1h period of dark or blue light (30 µmol·m^{-2} ·s^{-1}). Data are presented as mean of fluorescence intensity at 520 nm ± SEM (n = 30-50 cells). **p<0.01 (ANOVA test with Bonferroni correction). (B) Mean Ca^{2+} imaging traces of WT (black) and *phot* (red) exposed to an acute stimulation with blue light (30 µmol·m^{-2} ·s^{-1}) and recorded in Ca^{2+}-free condition. Representative calcium signals

observed at indicated time points (a and b from left traces) are shown on the right. *$p<0.05$ (Student's *t* test with Bonferroni correction).

4.3.2. Cytosolic IP_3 concentration is increased after blue light exposure

IP_3 is an important second messenger that is generated from the clivage of membrane phosphatidyl-D-inositol 4,5-bisphosphate (PIP_2) by the PLC. The importance of phospholipid signaling in plants has recently been reviewed (Munnik et al., 1998). Formation of IP_3 was reported to be involved in the blue-light-induced leaflet movements of Samanea saman, where the induction of IP_3 formation by blue light has been demonstrated (Kim et al., 1996). Moreover, considering that our results suggested the possible involvement of Ca^{2+} release from the ER and that IP_3R is the most ubiquitous ER Ca^{2+} channel, I carried out measurement of IP_3 concentrations in *Chlamydomonas* upon blue light exposure.

Cisbio IP-1 assays detect the accumulation of inositol monophosphate (IP-1), a stable downstream metabolite of IP_3 induced by activation of PLC cascade (Garbison et al., 2004). We observed the IP-1 accumulation was almost completely abolished in *phot* mutant either exposed to low light or blue light (Fig 14B). We determined WT samples exposed to blue light showed a higher accumulation of IP-1 compared to samples exposed to low light, suggesting an increase in IP_3 generation triggered by blue light signaling (Fig 14C). Moreover, a similar phenomenon was observed for *LHCSR3.1* transcript level (Fig 14D).

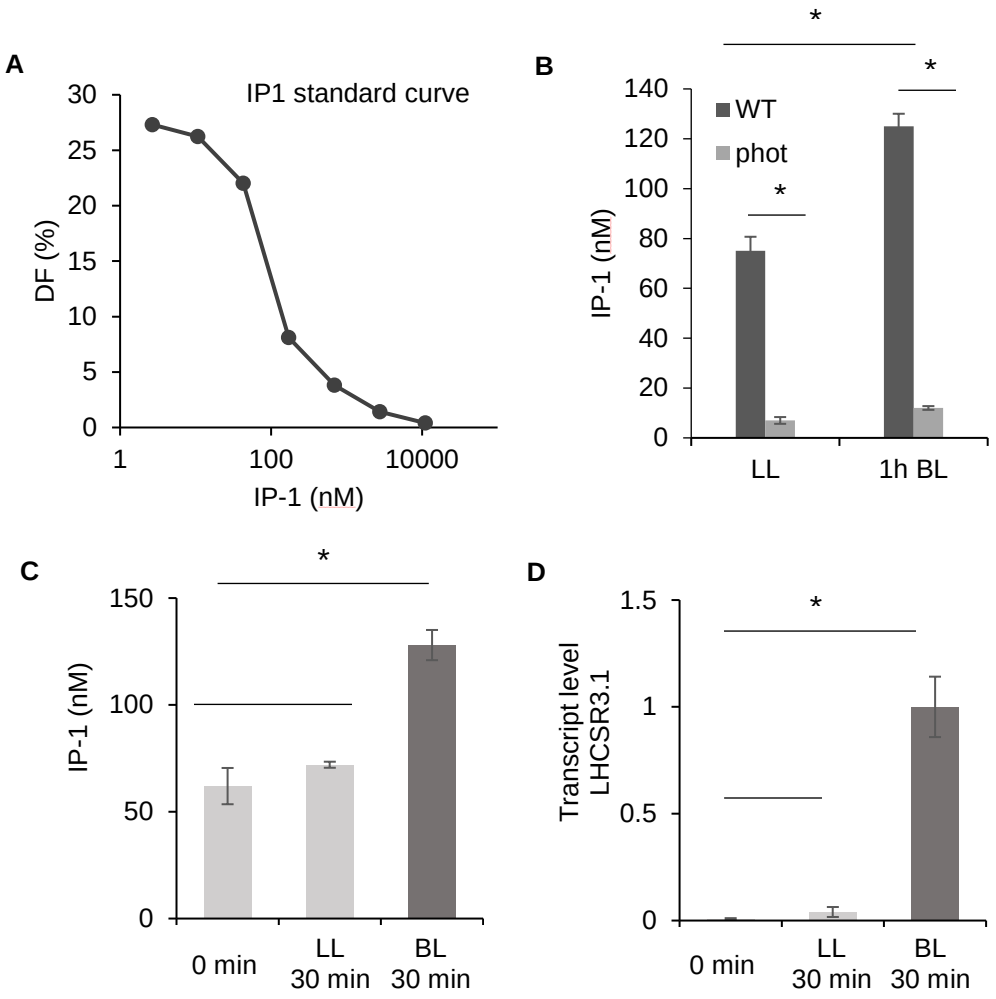

Fig. 14 Blue light exposure increases cytosolic IP_3 concentration. (A) Standard curve of IP-1 assay. Data are displayed in relation to the IP-1 standard curve. (B) *phot* mutant and WT cells were treated either 30 or 60 minutes with 100 µmol·$m^{-2}s^{-1}$ blue light. IP-1 accumulation measured by HTRF. Results shown are the mean +/- SEM of 3 independent experiments. (C) IP-1 accumulation of dark adopted cells either treated 30 minutes with LL (20 µmol·$m^{-2}s^{-1}$ white light) or 30 min BL (100 µmol·$m^{-2}s^{-1}$ 450nm). (D) *LHCSR3.1* transcript accumulation in WT cells with the same experimental condition as above was measured using qRT-PCR (n = 3 biological replicates; error bars represent SD). BL represents blue light and LL indicates low light samples.

4.3.3. The Ca^{2+}/CaM-dependent protein kinase inhibitor KN-93 blocks LHCSR3 expression

Calmodulin (CaM) is a Ca^{2+}-binding messenger protein which can modulate the activity of numerous Ca^{2+}-dependent proteins, including protein kinases such as CaM kinase II and phosphoprotein phosphatases such as calcineurin. It was previously reported that W7, a CaM inhibitor, strongly downregulates LHCSR3 gene expression (Maruyama et al., 2014) and that CaM kinases are involved in a light-dependent response in plant cells (Lu et al., 1996). Therefore, we examined whether the signal for LHCSR3 induction could also be regulated by CaM via a Ca^{2+}/CaM-dependent protein kinase using specific inhibitor, KN-93 which disturbs the CaM binding to the CaM kinase II catalytic subunit (Sumi et al., 1991). In this study I only used KN-93 and determined light-induced *LHCSR3* gene expression was partially abolished by 5 µM KN-93 (Fig 15). This result suggests that Ca^{2+} activated CaM transmits the light signal for LHCSR3 induction through a Ca^{2+}/CaM-activated protein kinase.

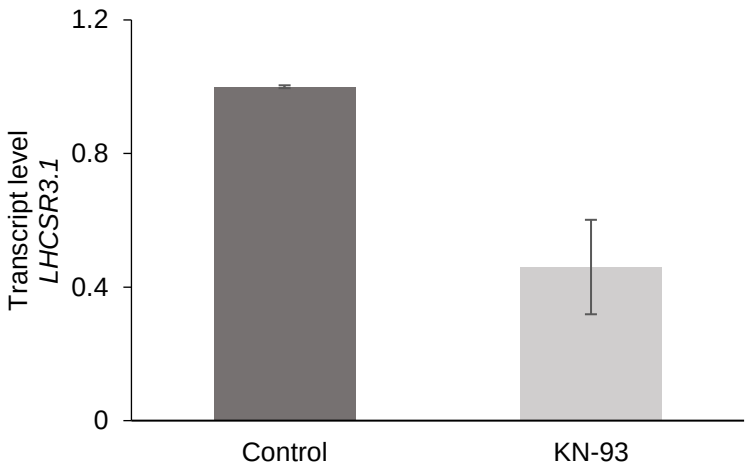

Fig 15 qPCR analysis of wild type cells treated with 5 µM KN-93 We treated *Chlamydomonas* wild type cells with 5 µM KN-93, a selective inhibitor of CaM kinase II in presence of 100 $\mu mol \cdot m^{-2} \cdot s^{-1}$ blue light and we determined KN-93 could repress LHCSR3.1 gene expression to 50%. Level.

4.3.4. Photosynthesis signals also modulate cytosolic Ca^{2+} levels

As Petroutsos et al. (2016) reported, the photosynthetic electron transport rate (ETR) in *phot* mutant cells is lower than in wild-type, although still higher in HL than in LL. Accordingly, we excluded the possibility that the diminished ETR observed in *phot* cells was the cause of the impaired LHCSR3 accumulation. Therefore, we believe that there are two different signaling pathways regulating LHCSR3 expression and that these two pathways share a common mediator, Ca^{2+} signaling. According to our hypothesis, in the presence of light, photosynthesis activity (ETR) leads to efflux of Ca^{2+} from the chloroplast to the cytosol, thus raising cytosolic Ca^{2+} concentration. We repeated this analysis in our lab and results are shown in Fig 16 A, B and C demonstrating that DCMU blocks ETR which represses strongly LHCSR3 protein and mRNA level accumulation as well as qE induction. We suggest that DCMU indeed blocks efflux of Ca^{2+} from the chloroplast to the cytosol which in turn lower concentration of Ca^{2+} in cytosol and inhibition of induction of *LHCSR3* gene expression. IBMX (3-isobutyl-1-methylxanthine- non-competitive selective phosphodiesterase inhibitor which raises intracellular cAMP), treatment was also not sufficient to recover LHCSR3 expression in the presence of DCMU, suggesting that the photosynthesis pathway is independent of cAMP signaling pathway.

Moreover, as Fig 16D and E show, DCMU could inhibit elevation of cytosolic free calcium.

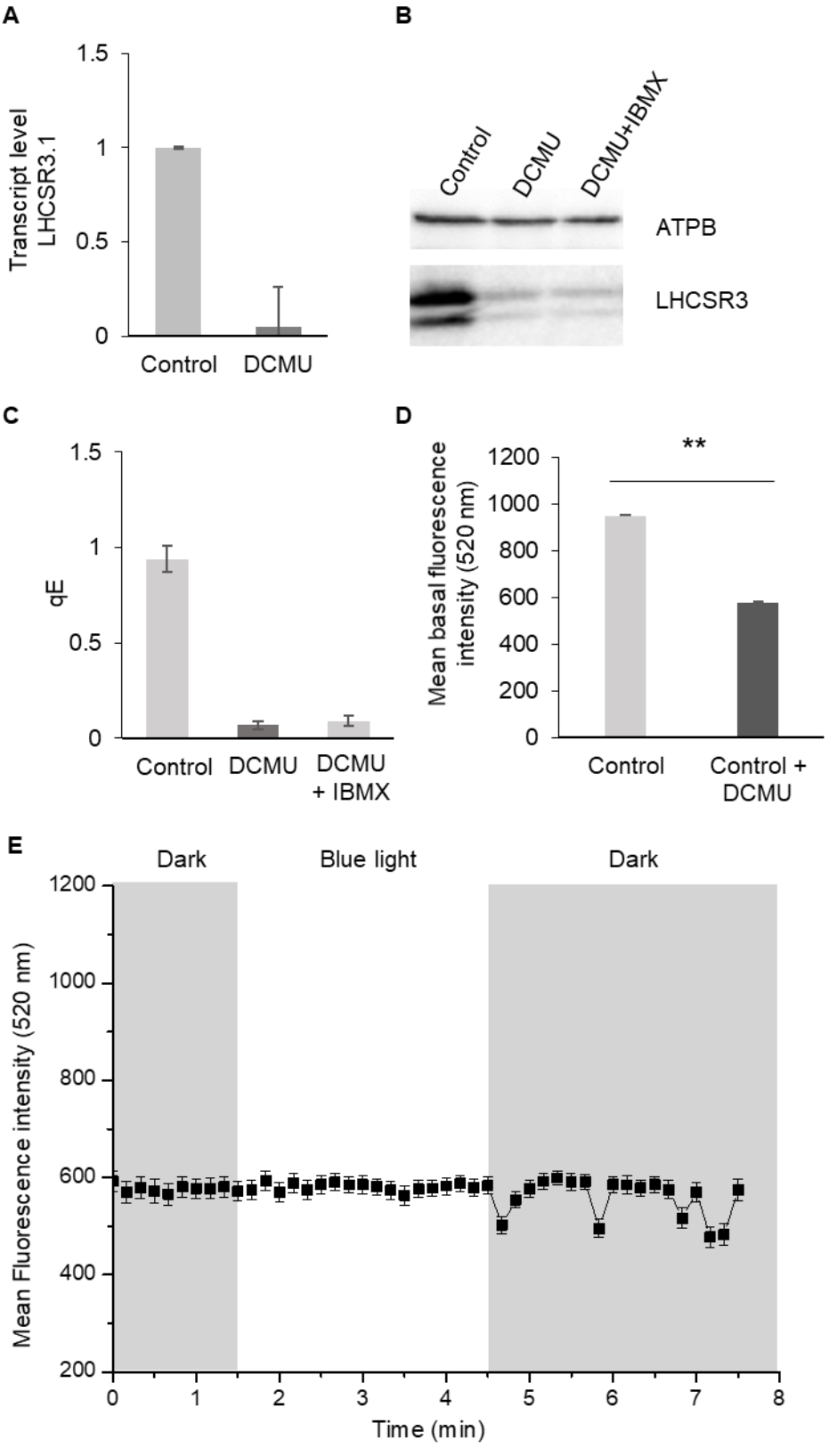
A
Transcript level LHCSR3.1
1.5
1
0.5
0
Control
DCMU
B
Control
DCMU
DCMU+IBMX
ATPB
LHCSR3
C
qE
1.5
1
0.5
0
Control
DCMU
DCMU + IBMX
D
Mean basal fluorescence intensity (520 nm)
1200
1000
800
600
400
200
0
**
Control
Control + DCMU
E
Dark
Blue light
Dark
Mean Fluorescence intensity (520 nm)
1200
1000
800
600
400
200
0
1
2
3
4
5
6
7
8
Time (min)

Fig 16 Effect of DCMU on cytosolic Ca^{2+} levels. (A) *LHCSR3.1* mRNA accumulation in C137 wild type cells at 1hour incubation of 100 µ mol photons m^{-2} s^{-1} blue light was quantified in the presence and absence of the PSII inhibitor DCMU. (*n* = 6 biological samples, error bars represent SD) (B) Immunoblot analysis of LHCSR3 accumulation in C137 cells after 3h exposure to 100 µ mol photons m^{-2} s^{-1} blue light in the presence and absence of 5 µM DCMU and 1mM IBMX. (C) qE value of samples with similar experimental condition of A and B. (D) mean basal cytosolic Ca^{2+} levels of WT treated or not with 5 µM DCMU prior to a period of blue light (1 h, 30 µmol photons m^{-2} s^{-1}). (E) Mean Ca^{2+} imaging traces of WT treated with 5 µM DCMU, exposed to an acute stimulation with blue light (30 µmol photons m^{-2} s^{-1}) and recorded in calcium-free condition. Data are presented as mean of fluorescence intensity at 520 nm ± SEM (n = 30-50 cells). **p<0.01 (Student's *t* test).

4.3.5. cAMP role on Phot-dependent LHCSR3 regulation

As described briefly in introduction, Petrotsus et al (2016) proposed that second messengers such as the cyclic nucleotides cAMP or cGMP act as the signaling molecules downstream of PHOT. They observed that the treatment of *phot* cells with an inhibitor of cAMP and cGMP phosphodiesterases, IBMX, rescued LHCSR3 expression suggesting that cyclic nucleotides are involved in the regulation of LHCSR3 expression (Petroutsos et al., 2016).

Therefore, to elucidate more in details one of the downstream elements of PHOT, we analyzed the role of cAMP on cytosolic calcium level. As a first step, we confirmed the results obtained from Petrotsus and colleagues as shown in Fig 17 A and C. Briefly, qE induction as well as LHCSR3 protein accumulation in wild-type and *phot* cells treated with 1 mM IBMX for 24h at 100 µmol photons m^{-2} s^{-1} blue was evaluated and demonstrated in presence of IBMX which leads to accumulation of cAMP, qE level as well as LHCSR3 protein accumulation were rescued to wild type level. Furthermore, we observed differences in basal cytosolic Ca^{2+} levels of *phot* mutant cells in the presence of 1 mM IBMX between different times of treatment. In one-hour incubation of *phot* cells with IBMX in presence of blue light, cytosolic Ca^{2+} level dropped significantly. However, after an overnight incubation with same drug, basal calcium level increased to a level

higher than the one observed for non-treated cells. Further analysis will be needed to clarify the exact function of cAMP on cytosolic Ca^{2+} level as well as LHCSR3 regulation.

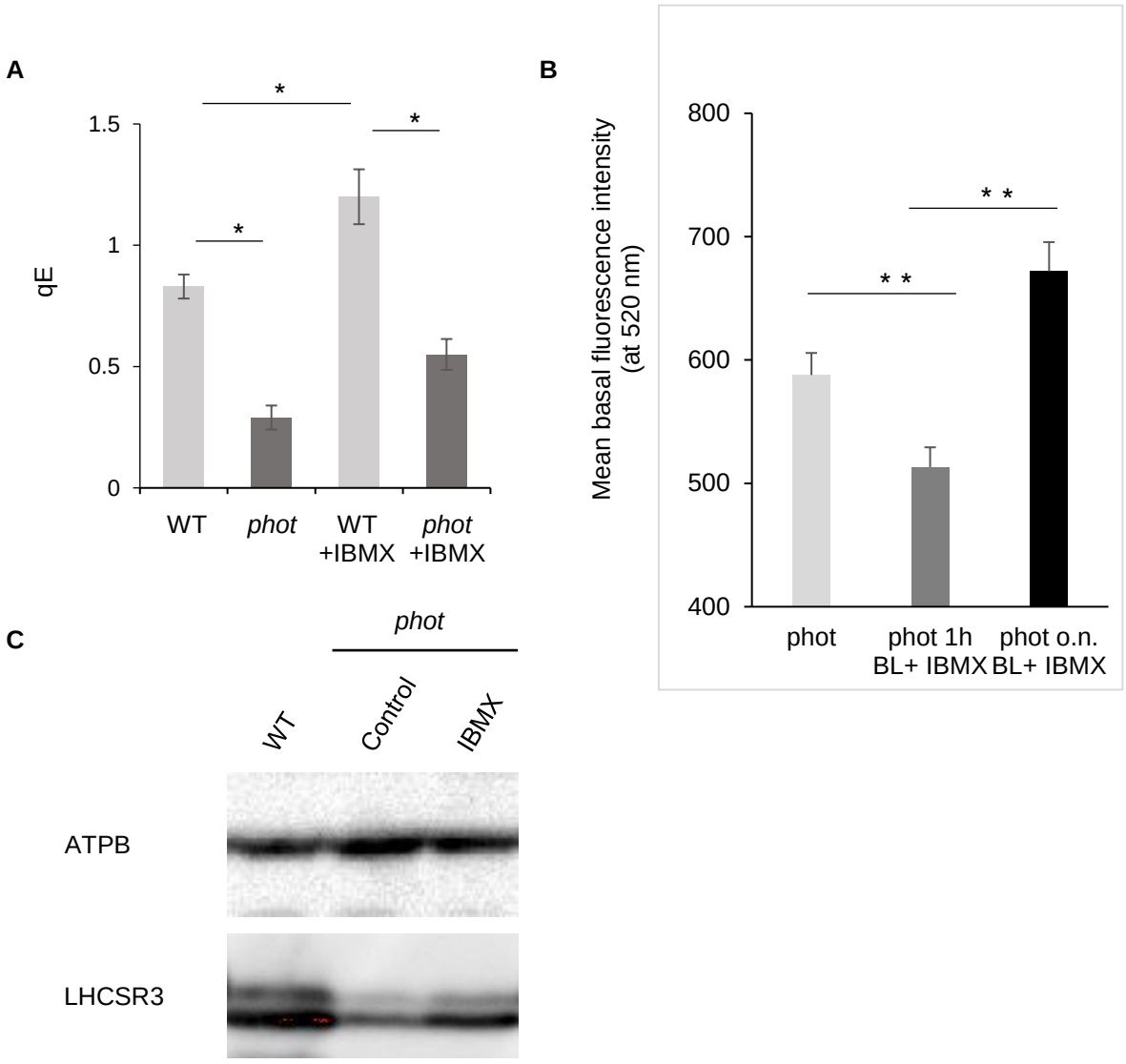

Fig 17 cAMP regulates LHCSR3 expression via Phot-dependent Ca^{2+} signaling. (A) qE induction in wild-type and *phot* cells treated with 1mM IBMX for 24h at 100 µmol photons m^{-2} s^{-1} blue. (B) Basal cytosolic Ca^{2+} levels of *phot* cells incubated either 1h (*phot* 1h BL+ IBMX) or overnight (*phot* o.n. BL+ IBMX) with 1mM IBMX in presence of 100 µmol photons m^{-2} s^{-1} blue (*n* = 3 biological samples; error bars represent SD). (C) LHCSR3 accumulation in WT and *phot* mutant treated or not with the phosphodiesterase inhibitor IBMX (ATPB is the loading Control) with the same experimental condition.

4.3.6. The role of IP_3R in the Ca^{2+}-dependent LHCSR3 regulation

IP_3 is a second messenger used by many cell types to release Ca^{2+} from internal stores. In order to further explore the contribution of the IP_3R to intracellular Ca^{2+} signals, we used a selective receptor blocker. The macrocyclic bis-1-oxaquinolizidine alkaloid Xestospongin C (XeC), a metabolite isolated from the Australian sponge Xestospongia species, is well characterized as a potent blocker of the IP_3R. We determined that mRNA abundance of LHCSR3.1 was strongly repressed when cells treated with 5 μM XeC in presence of 1 h blue light (100 μmol photons m−2 s−1) (Fig 18).

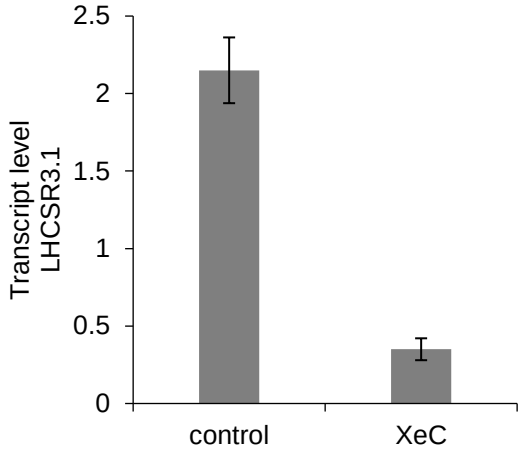

Fig 18 Quantitative real-time RT-PCR analyses of the *LHCSR3.1* transcript level treated with XeC in presence of 1h blue light Chlamydomonas wild type cells irradiated 1 h with 100 μmol m^{-2} s^{-1} blue light. DMSO (denoted as Control), 5 μM XeC was supplemented prior to the high light exposure. Mean values shown with s.e. (n = 3)

Moreover, I demonstrated that blue light can increase cytosolic Ca^{2+} level for the cells preincubated in low light overnight and this elevation is inhibited very strongly in the presence of 5 μM XeC (Fig 19).

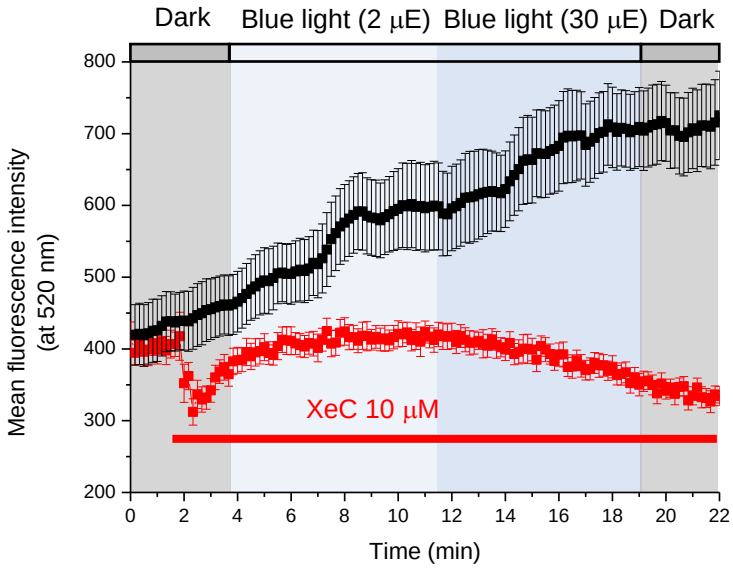

Fig 19 The effect of dim or strong blue light and Xestospongin C (IP_3R specific blocker) on cytosolic calcium level Graph shows either dim or stronger blue light can stimulate and raise cytosolic calcium level and this elevation was inhibited very strongly in presence of 10 μM xestospongins C.

We ordered two insertional mutants named LMJ.RY0402.257156 and LMJ.RY0402.202516 (Hereafter named *ip3r-156* and *ip3r-516* respectively) generated by the Chlamy Library project (https://www.chlamylibrary.org/) (Li et al., 2016). Briefly, mutants were generated by electroporation of a DNA cassette (CIB1) conferring resistance to paromomycin into the *Chlamydomonas* strain CMJ030. We confirmed insertional site by PCR (Fig 20 A). I followed the same experimental method I used at fig 18 by treatment the cells with 1h blue light but unexpectedly I only could see nearly 40% of *LHCSR3.1* mRNA reduction in comparison with wild type cell as shown in Fig 20B. This sparks controversy because if we assume IP_3R is the central key factor of cytosolic calcium regulation of LHCSR3, 40% of mRNA reduction doesn't fully support the involvement of IP_3R. I explain my interpretation for this controversial result at final discussion.

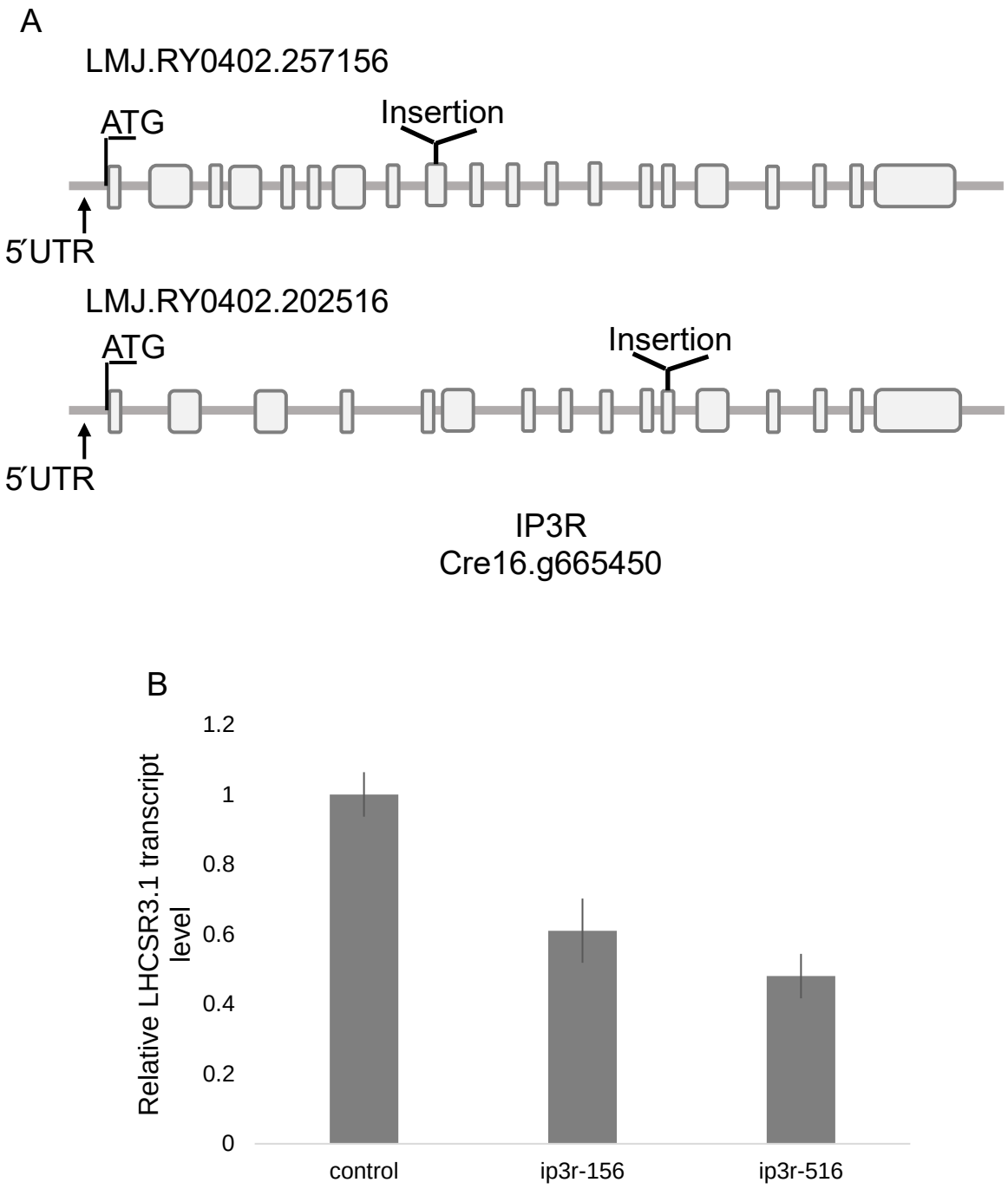

Fig 20 Characterization of *ip$_3$r* knock out mutants. Phenotype of two ip$_3$r mutants which have a single tag insertion in different exons (A) were analyzed by quantification of LHCSR3.1 mRNA by exposure to 1 h 100 µmol m^{-2} s^{-1} blue light (B). PCR analysis confirmed *ip$_3$r*-156 and ip3r-516 have single insertion on base 3090387 and 3097263 phytozome (genome v5.5) respectively.

4.3.7. Red light has no effect on cytosolic Ca^{+2}

In Accordance with our hypothesis that both signals form photosynthesis machinery as Ca^{+2} efflux to cytosol and IP_3 from PHOT activation is needed to activate and open IP_3R channel, we could dissect those two signals by applying red light. Red light which can only activate chlorophyll in photosynthesis machinery but not PHOT can give us a better cue how those two pathways are involved. With considering only photosynthesis signal can be activated by red light, we expect to not see elevation of cytosolic calcium level even though with higher intensity of red light and so we observed that as Fig 21 show clearly.

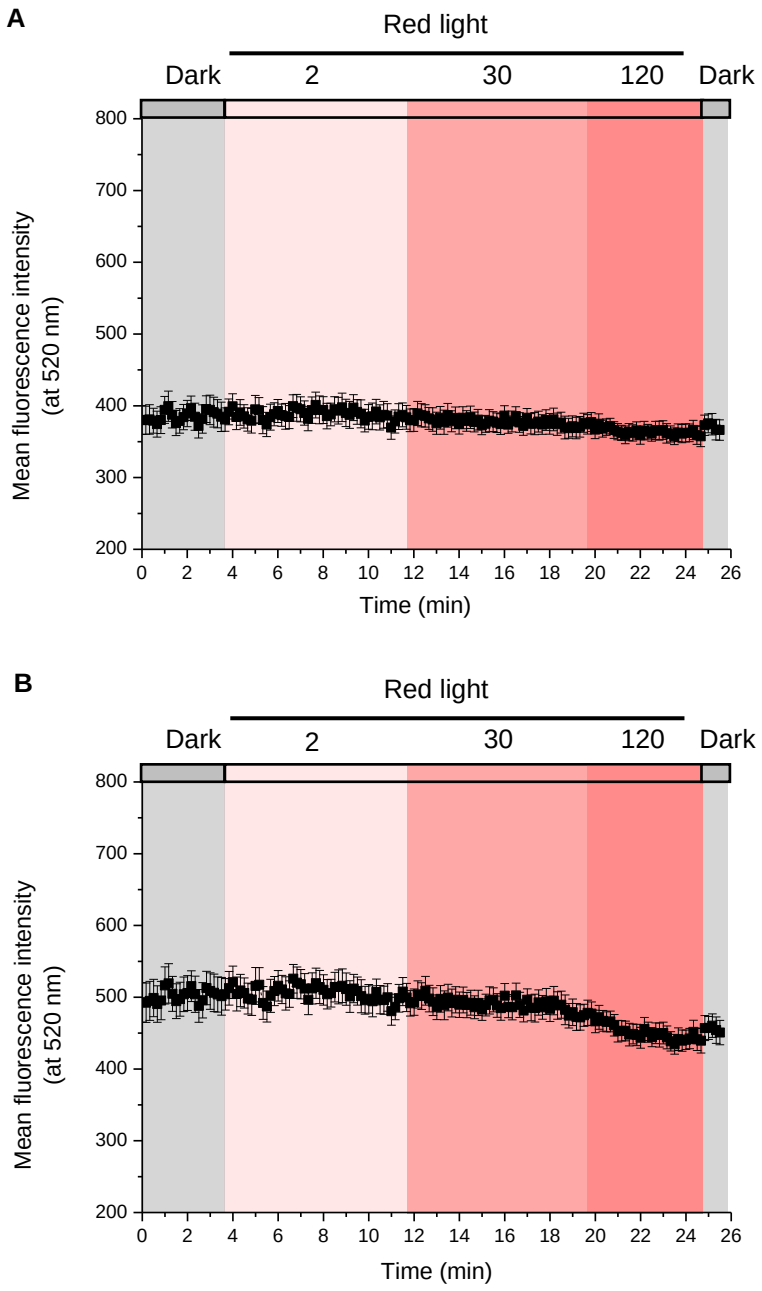

Fig 21 Red light didn't exhibit a response to Ca^{2+} levels. Mean Ca^{2+} imaging traces of WT cells to a dim (2 µmol·m^{-2}·s^{-1}), weak or strong (30 or 120 µmol·m^{-2} ·s^{-1} respectively) red light recorded in calcium-free condition after an 1h period of dark A or red (30 µmol·m^{-2} ·s^{-1}) (B). Data are presented as mean of fluorescence intensity at 520 nm ± SEM (n = 30-50 cells). **p<0.01 (ANOVA test with Bonferroni correction). *p<0.05 (Student's *t* test with Bonferroni correction).

4.4. Discussion

1 Phototropin activation triggers cytosolic calcium signaling

Our results depicted in Fig 13 show both basal level of cytosolic Ca^{2+} treated with 1-hour illumination with blue light or Ca^{2+} imaging traces of cells exposed to an acute stimulation with blue light were elevated only in wild type cells bot not *phot* mutant. Thus, we can conclude that blue light-dependent Ca^{2+} signaling is under regulation of phototropin.

2 IP_3 is involved in activation of $[Ca^{2+}]_{cyt}$

IP_3 is also known to cause the release of Ca^{2+} from internal stores across non vacuolar membranes in plants while it was also suspected to mediate mobilization of Ca^{2+} from the ER upon PLC activation in *C. reinhardtii* (Kuin et al., 2000).

Our results show that blue light can stimulate IP_3 production in WT cells, however in *phot* mutant IP_3 accumulation under blue light was not observed suggesting that phototropin regulates PLC-catalyzed IP_3 formation.

3 cAMP-dependent induction of LHCSR3 expression involves intracellular Ca^{2+} signaling

As described, Petrotsus et al. (Petroutsos et al., 2016) found a link between PHOT-dependent Ca^{2+} signaling and cAMP, that we were able to reproduce. These results are not in contradiction with the involvement of phosphoinositides pathway. Indeed, there is numerous evidence for a physiological interaction between the phosphoinositides and cAMP signaling pathways. Both IP_3 and diacylglycerol, products of PLC activation, affect cAMP formation. Ca^{2+} mobilized from intracellular stores by IP_3 forms a complex with CaM and the Ca^{2+}-CaM complex can directly bind to certain forms of adenylyl cyclases to activate them. On the other hand, there are also several reports that show that the hydrolysis of PIP2 is regulated by cAMP and cAMP-dependent protein kinase A (PKA). Therefore, we can easily imagine a crosstalk between PKA and PLC signaling pathways ultimately leading to intracellular Ca^{2+} increase and LHCSR3 expression. Further analysis will be necessary to characterize the exact function of cAMP PHOT-dependent Ca^{2+} signaling.

4 Photosynthesis signals are involved in activation of intracellular Ca^{2+} signaling

This will be further explained in final discussion.

5 The IP_3R on the ER membrane is involved in the regulation of intracellular Ca^{2+} signaling

Although XeC which is a specific inhibitor of IP_3R in mammalian cells could inhibit strongly *LHCSR3.1* mRNA abundance as well as *Chlamydomonas* cytosolic calcium level stimulated by blue light but we couldn't observe a strong downregulation of *LHCSR3* gene expression as shown in Fig 20 by *ip3r* knock out mutants. However, the possible reason for this contradiction and possible future experiment for this section is described further in final discussion.

Chapter 5

Forward genetic approach to identify genes involved in the calcium dependent light stress response

5.1. Summary of work

In green algae, a strong light intensity leads to harmful overexcitation of the photosystems. Light-harvesting complex stress-related protein (LHCSR3) is responsible for a quick response energy dependent quenching (qE) in *Chlamydomonas reinhardtii*; however, regulation of *LHCSR3* gene expression is as yet fully understood. To address those questions, a high throughput forward genetic approach was used to screen mutants using bioluminescence derived from a luciferase reporter gene under various light cues. Screening strategy was aimed to isolate and identify genes involve in blue light dependent regulation of LHCSR3 via calcium signaling. 7000 transformants were screened and at the first step those transformants which had *severe growth* deficiency in calcium-depleted medium under continuous strong blue light were chosen. For second step of screening, qE value and LHCSR3-LUC activity of chosen transformants were measured and those show very low or high values were selected for further characterization and sequencing analysis. 9 mutants have been isolated that exhibit defect in calcium signaling pathway(s), blue-light-dependent signaling and photosynthetic electron flow. We focused on mutant in this study has insertion in *CPLD62* gene. CPLD62 predicted to have LETM1 domain which previous research in mammalian cells showed that LETM1 participated in mediating mitochondria Ca^{2+} influx or efflux. The recent report showed that CPLD62 protein is localized in Chloroplast (Terashima et al., 2010). In our research we investigate the possible Ca+2/H+ activity of LETM1 in thylakoid membrane and its possible connection to CAS protein. Our results present a broader image about the interplay between different signaling pathways to regulate *LHCSR3* gene expression.

5.2. Brief introduction

Calcium signaling as described in previous chapters is very important for survival of cells under environmental stress conditions (Boyce and Yuan, 2006; Chihiro and Katsuhiko, 2017; Knight, 1999); therefore, I assumed if we eliminate important calcium signaling factors, cells probably become highly photosensitive against high light stress. To examine my hypothesis, I treated *Chlamydomonas* wild type cells with several well know mammalian or plant calcium signaling blocker reagents such as W7 (Calmodulin blocker), XeC (IP_3R) or depleted of free calcium ion by titration with ethylenebis (oxyethylenenitrilo) tetra acetic acid (EGTA), and I could observe only

those cells treated with W7, XeC or EGTA under 100 µmol m-2 s-1 blue light but not red light were eventually died and couldn't growth properly (Data are not shown). Moreover, the experiences and knowledge I received from chapter two helped me to design a high throughput forward genetic approach using random insertional mutagenesis to pinpoint important genes involved in calcium signaling downstream of PHOT. For this purpose, I designed a three-step screening method as shown in Fig. 22 for proceeding with my forward genetic approach. In this strategy I supposed those mutants defects in important calcium signaling factors cannot survive under strong blue light. However, since calcium signaling is a quick responsive process, a reporter strain which can quickly show transcriptional or translational behavior of LHCSR3 gene was essential. Therefore, to facilitate study of LHCSR3 gene expression, I developed a monitoring system for LHCSR3.1 gene expression in *Chlamydomonas* by fusion of LHCSR3 promoter with luciferase gene as reporter and transform it in C137 wild type cell to generate a reporter strain for proceeding with my forward genetic strategy.

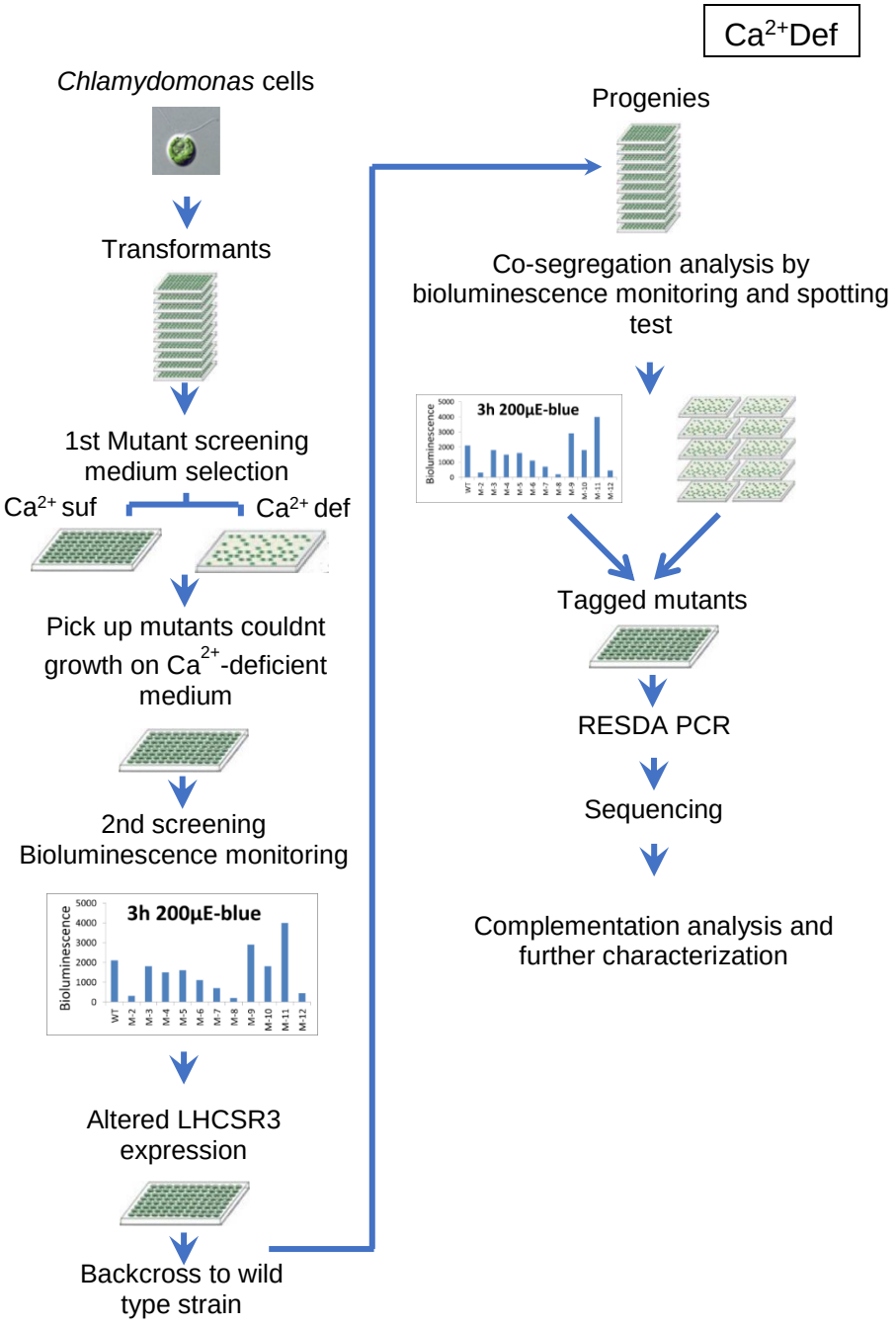

Fig 22 Forward genetic strategy to identify novel calcium signaling components involved in LHCSR3 regulation. This strategy is based on screening mutants in calcium deficient medium under strong blue light irradiation wherein those mutants impaired in important cytosolic calcium signaling pathways are not able to induce LHCSR3, therefore sensitive to strong blue light and prone to cell death. Ca^{2+}suf (Ca^{2+} sufficient) medium has usual calcium concentration in Sueoka medium (68 µM) and Ca^{2+} def (Ca^{2+} deficient) medium has lower calcium concentration than in Sueoka medium (14 µM).

5.3. Results

5.3.1. Screening of candidates for a high-throughput assay of bioluminescence reporter strain

Initially we measured the bioluminescence of a reporter strain (*LHCSR3.1-lucCP*) that expresses the luciferase gene under the control of the *LHCSR3.1* promoter under high-throughput assay conditions developed for this study (see Materials and Methods). However, we failed to detect significant luciferase activity in all 2000 transformants. One of the possible problems could be an epigenetic silencing of transgene expression cassette by *Chlamydomonas* regulatory elements. Several articles have reported that when the first intron of a gene was inserted in the 5'-upstream regions of that gene, a several-fold enhancement of gene expression was observed (Hirochika et al.). Therefore, to overcome this problem, we fused the full LHCSR3 gene, including exons and introns, into the luciferase gene (Fig 23 A) and transformed this expression construct, as described in the methods chapter, into *Chlamydomonas* C137 wild type cells. In this set of experiments, I successfully isolated a clone which exhibited stable and robust luciferase activity by incubating the cells under high light conditions. Southern blot analysis revealed there was a single copy insertion of expression cassette in the genome of reporter strain (Fig 23 B).

I demonstrated that the bioluminescence activity of the reporter strain correlated well with the qE, endogenous *LHCSR3* gene expression, as well as the LHCSR3 protein accumulation pattern (Fig 24). Moreover, LHCSR3.1 showed rhythmicity under low light condition (Fig 25) which implies LHCSR3-LUC reporter bioluminescence system is such sensitive that we could determine its rhythmicity under dim blue light, but red light did not show this rhythmicity possibly due to inhibitory effect of red light on LHCSR3 mRNA abundance as fully described in chapter one. I named the candidate clone $A4^{+}$ and used it as a wild-type strain in this study.

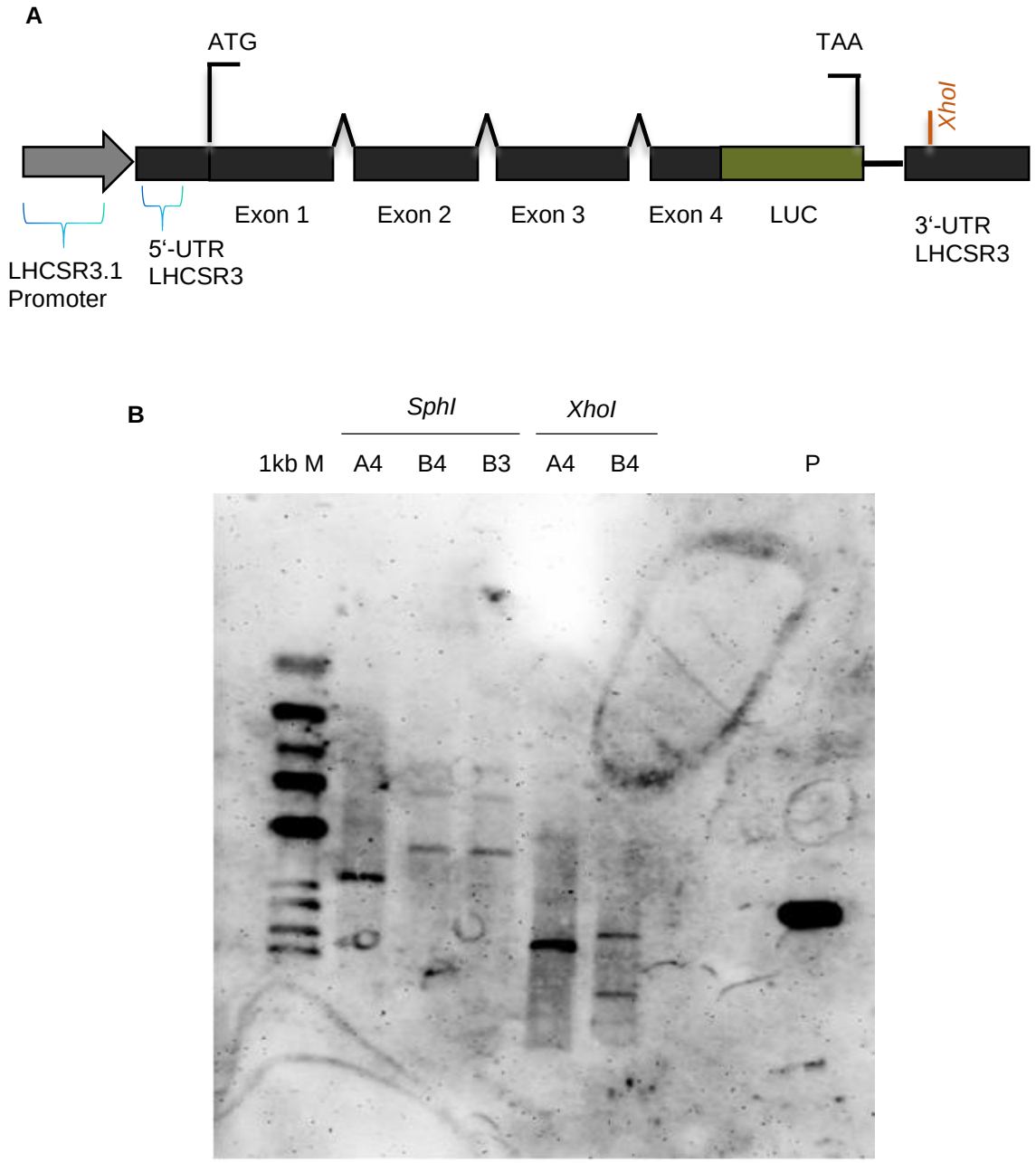

Fig 23 Transformation of LHCSR3.1-LUC expression cassette into C137c wild type cells to generate a reporter strain. A a schematic map of the LHCSR3.1-luc construct. B Southern blot analysis of C137c reporter strains A4, B3, and B4 digested separately with SphI & XhoI and P:pcr2.1TOPO-lucNCtag digested with BamHI as control. We chose A4 to proceed with our forward genetic analysis.

5.3.2. Characterization of the reporter strain

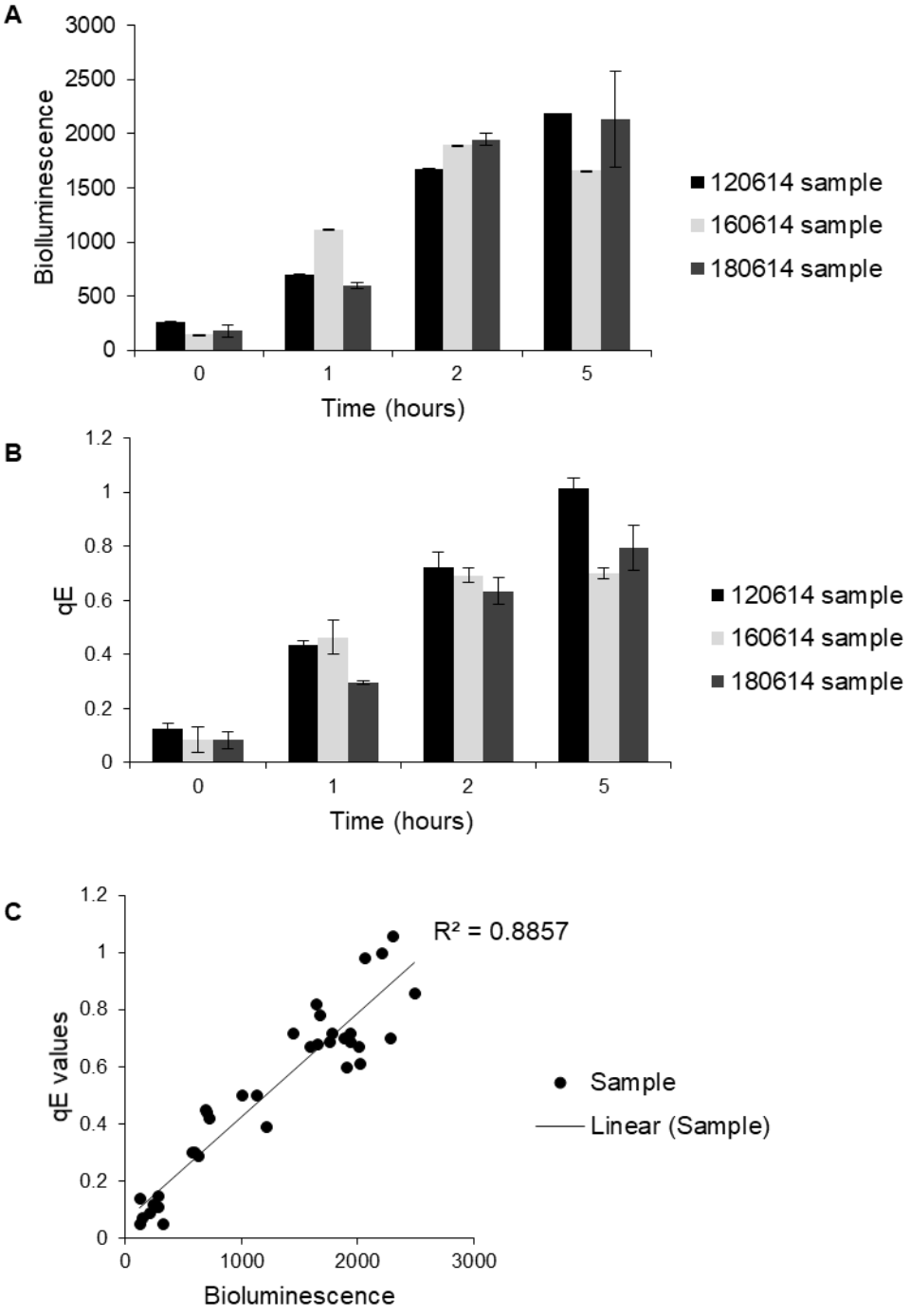

Fig 24 The positive correlation of qE values and bioluminescence activity. Low light adopted A4 reporter strain was subjected to high light for five hours and bioluminescence (A) as well as qE capacity (B) were measured at different time point and the datasets were compared via regression analysis in Excel (C). Each data point represents a mean of three biological replicates

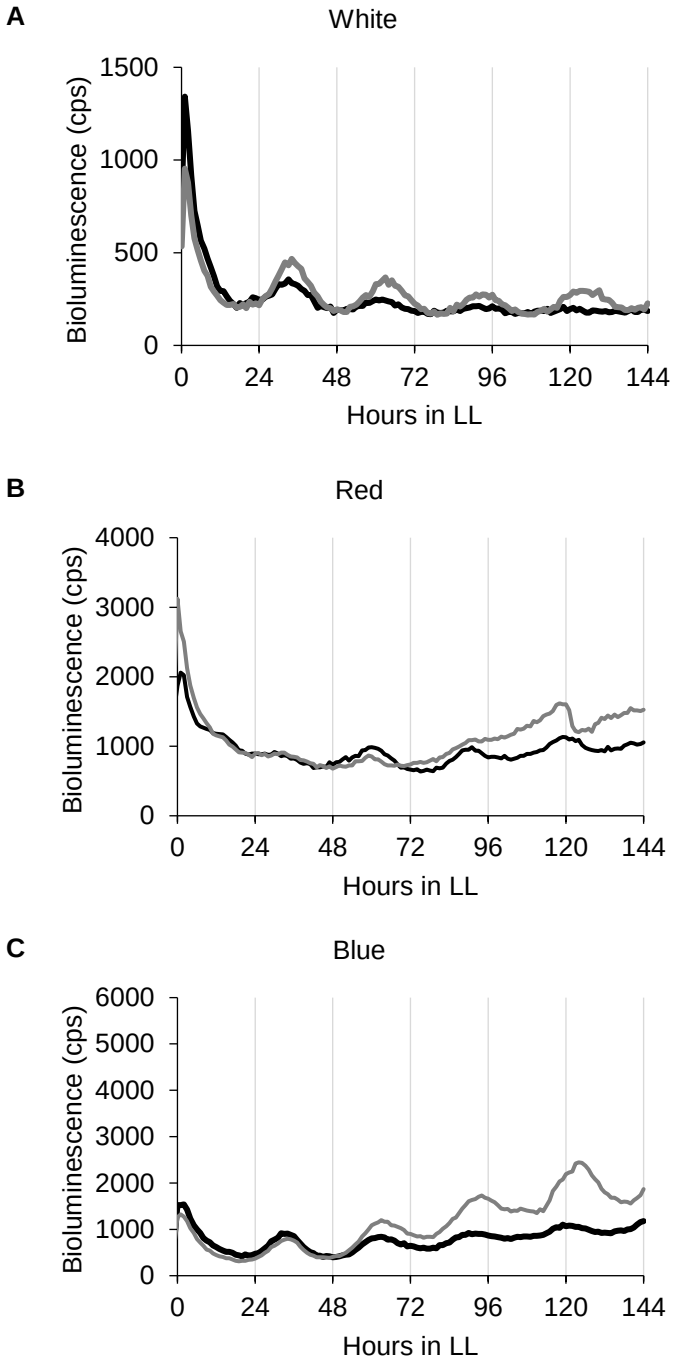

Fig 25 Representative bioluminescence traces of A4 reporter strain by a continuous culture system under 2 μmol photons m^{-2} s^{-1} of white, red or blue light incubation. LHCSR3.1-luc showed rhythmicity under white and blue but not red light.

5.3.3. Forward genetic approach

For *C. reinhardtii*, a wide range of molecular genetic approaches, including gene tagging with insertional mutagenesis by using an indexed genomic library, are reported (Tam and Lefebvre, 1993; Vallone et al., 2004). Our bioluminescence reporter strains will enable the same forward genetic approach to pinpoint regulatory elements involved in regulation of *LHCSR3* gene expression.

To generate insertional mutants, the $A4^{+}$ strain was transformed with a DNA fragment containing a hygromycin-resistant gene (Berthold et al., 2002). We screened ~7,000 transformants which could grow on hygromycin plates and subjected them to a three-step screening (Fig 22) wherein at the first step of screening as described above by growing them in HS calcium-deficient medium in 96 well plates under strong blue light stress at 100 µmol m-2 s-1. High salt medium according to Sueoka method has ~ 68 µM $CaCl2.2H_2O$ as described in method; however, for preparing calcium deficient medium, I used almost five times less concentration of calcium (~ 14 µM) without any other modification in recipe. I chose those mutants which showed impairment in photoautotrophic growth. For the second step of screening, I isolated 12 candidate mutants which showed either very high or very low bioluminescence, Then, 91% of the candidates (11 mutants) that reproduced their mutant phenotypes were analyzed for qE measurement. Next, all the mutants were backcrossed to the $A4^{-}$ strain, and progenies were subjected to bioluminescence measurements and hygromycin resistance testing (cosegregation analysis) (Fig 4). If the mutation was caused by a single integration of the marker gene into the genome, the mutant phenotype should have strictly cosegregated with the hygromycin resistance. Five mutants showed strict cosegregation. On the other hand, if the integration occurred at multiple loci, only a proportion of hygromycin-resistant progeny (~50% if integration occurred at two loci) should have exhibited the mutant phenotype. Thus, “partial cosegregation” was observed, was seen in two mutants. Furthermore, 7 mutants demonstrated mutation was independent from the integration of hygromycin resistant cassette (Data are not shown).

5.3.4. Systematic identification of the responsible genes

To identify integration sites of the marker gene, we determined flanking genomic sequences by the restriction enzyme site-directed amplification (RESDA-PCR). I analyzed 5 mutants tagged by

a single integration of the marker gene. I succeeded in identifying flanking genomic sequences on both sides of the marker gene in those mutants. The rate of success in identification of both flanking sequences was high in mutants generated with 20 ng of transforming DNA. With higher concentration of transforming DNA (300ng) I got few mutants with amplification only of the marker sequence, probably because of the integration of concatemeric marker DNA. Flanking sequences were compared with the *Chlamydomonas* genome sequence (Phytozome *Chlamydomonas reinhardtii* version v12: https://phytozome.jgi.doe.gov/pz/portal.html. All of the flanking sequences were found in the database. In all five mutants, the marker genes were integrated without any large changes in their original genome sequences. The candidate genes are listed in Tables 6. Based on the annotation of the genome sequence (Phytozome *Chlamydomonas reinhardtii* version 12.0), sequence similarity to known proteins, or conserved functional domains, I realized most of the mutations were involved in calcium signaling in *Chlamydomonas*, showing that my screening strategy was successful to identify calcium signaling related genes. For further characterization of identified mutants, I measured qE capacity value of WT and mutant cells incubated 8 hours with I focused on the P14 mutant which in phytozome v12 described as Cre12.g538700 CPLD62 Leucine zipper-EF-hand containing transmembrane protein.

Table 6: List of mutants were isolated and identified from screening of 7000 transformants

Mutant ID	Target gene	Feature	Best hit
P14	Cre12.g538700	CDS	CPLD62, LETM1
P16	Cre01.g016750	5‘UTR	PSBS2
P18	Cre03.g193450	Promoter	IQ calmodulin-binding motif with GTPase domain
P33	Cre03.g188700	CDS	Plastid lipid associated protein, Fibrillin, PLAP6
P35	Cre03.g188700	CDS	Plastid lipid associated protein, Fibrillin, PLAP6
P42	Cre06.g263600	CDS	Apoptosom with calcium channel domain

Table 7: qE value of isolated mutants after 8 hours irradiation with high light (100 µmol m^{-2} s^{-1} blue light)

Mutant ID	low light*	high light
WT	0.08 +/- 0.003	0.8 +/- 0.1
P14	0.2 +/- 0.01	1.2 +/- 0.2
P16	0.03 +/- 0.09	0.4 +/- 0.07
P18	0.1 +/- 0.01	0.36 +/- 0.04
P33	0.07 +/- 0.01	0.6 +/-0.14
P42	0.13 +/- 0.04	0.3 +/- 0.02

*low light: 8 hours irradiation with 15 µmol m^{-2} s^{-1} white light

5.3.5. P14 showed higher accumulation of LHCSR3 and lower growth rate in exposure to blue light

We analyzed qE values as well LHCSR3 protein accumulation of P14 mutant cells treated 4 days with 100 µmol m^{-2} s^{-1} blue light and the observed P14 cells exhibited a significantly higher qE value as well as LHCSR3 protein accumulation after 8 hours of light treatment (Fig 26A&B), and this higher value lasted for 1 day. As described in previous chapter, cAMP is reported to be possibly involved in *LHCSR3* regulation via phototropin pathway; therefore, we analyzed whether high accumulation of LHCSR3 in p14 mutant can be affected by cAMP-PHOT pathway. Our result showed no effect of 1mM IBMX on LHCSR3 accumulation in P14 cells with the same experimental condition of Fig 26 A&B.

Both NCBI and SMART protein structure prediction shows CPLD62 has LETM1 domain near the end of the C terminus. Hereafter, I name our isolated and identified mutant as *letm1*. PCR analysis confirmed that *letm1* has a single insertion in ATG start codon after AT bases. AT-G.

However, when we prolonged blue light incubation time, we observed *letm1* (P14) mutant cells exhibited extreme photosensitivity after one day and Fv/Fm levels drop strongly in mutant but not in wild type cells. And at the end of fourth day, nearly all mutant cells did not survive in this condition but not wild type cells. In Fig 27 I show the track of Fv/Fm and cell growth changes during 4 days of 100 µmol m^{-2} s^{-1} blue light incubation.

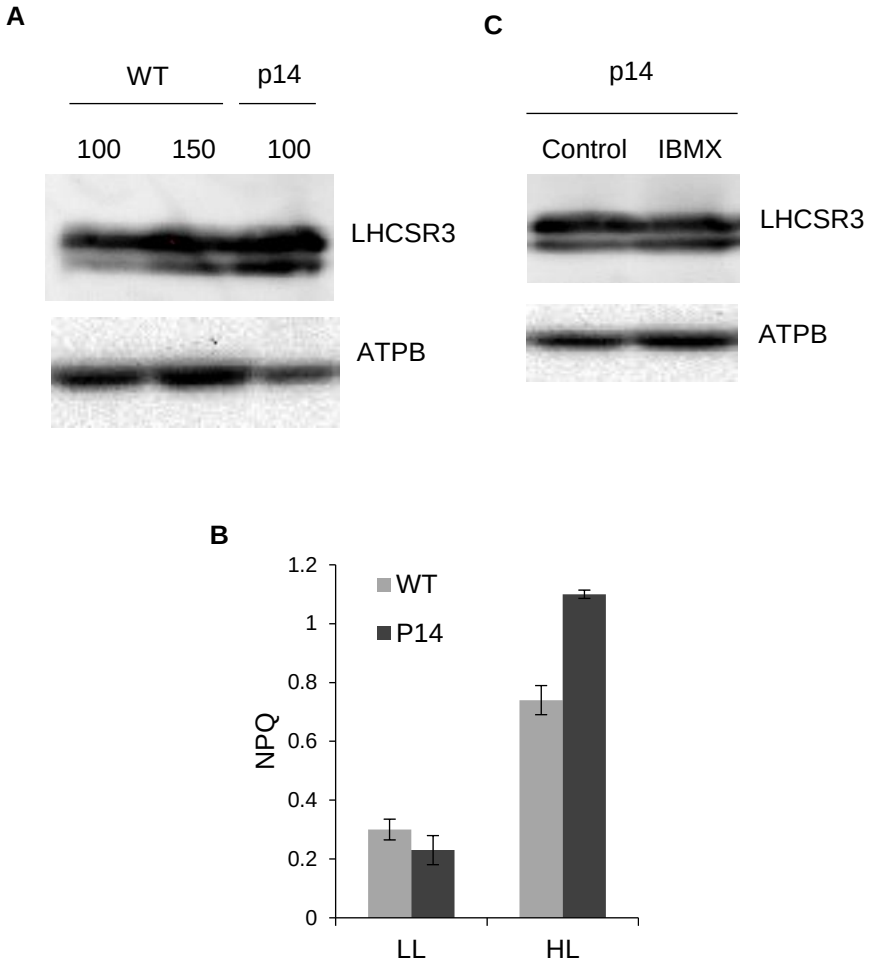

Fig 26 Characterization of P14 mutant and WT cells. (A) Quantification of LHCSR3 protein amounts in total cell extract from the wild type and P14 knock out cells. Cells were grown in HS medium under 8 hours with 100 µmol m^{-2} s^{-1} blue light upon SDS-PAGE fractionation and immunoblot analysis. (B) NPQ capacity of the same cells used in Fig 26A. (C) 1mM IBMX treatment of WT and P14 mutant cells with the same experimental condition as Fig26A.

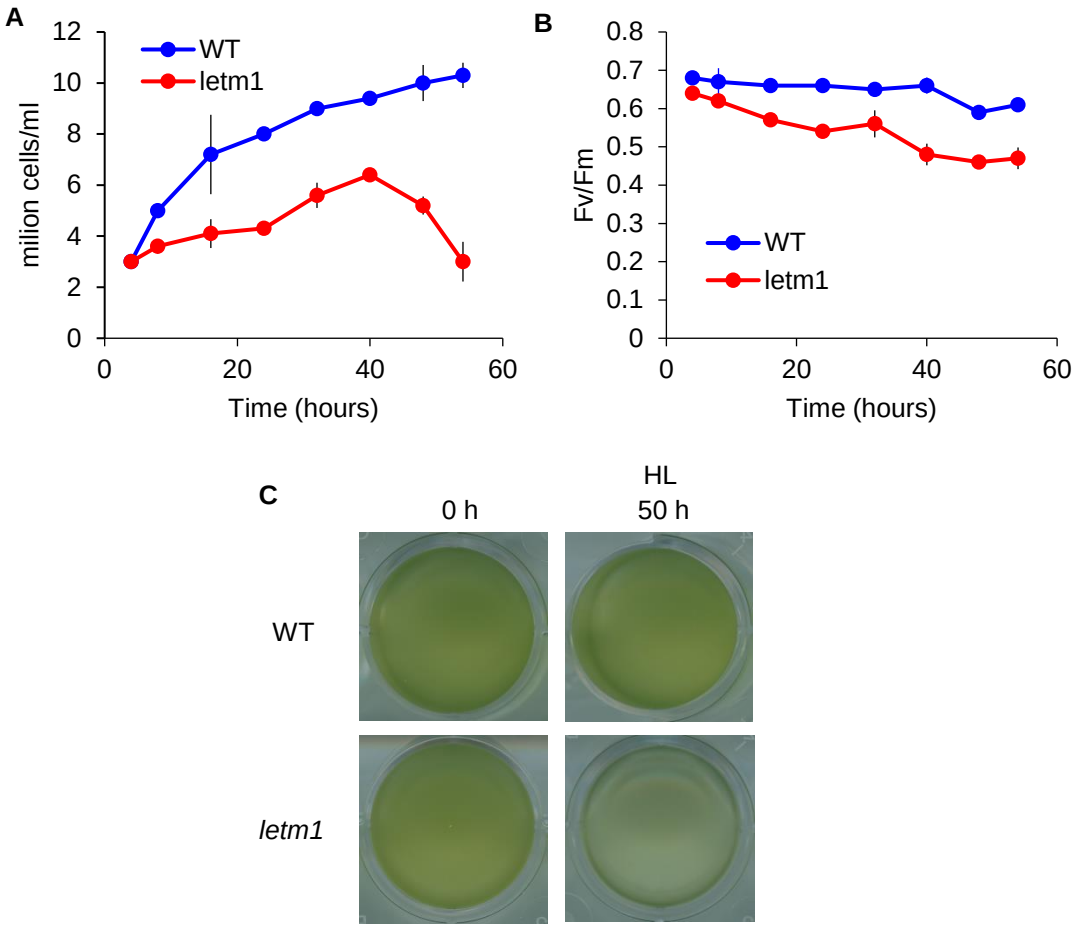

Fig 27 Photoautotrophic growth of *letm1*mutant and the parental WT. (A) growth rate tracking of *letm1* and WT cells incubated in 12-well plates with shaking for 60 hours under 100 µmol photons $m^{-2} \cdot s^{-1}$ blue light (450nm). (B) Tracking the maximum quantum efficiency of Photosystem II (Fv/Fm) of the same samples indicated in Fig27A and (C) photographic images of the same cultures of Figure 27A considered as 0h (before blue light treatment) and HL (100 µmol photons m^{-2} s^{-1} blue light).

5.4. Discussion

As has been shown in Fig 30, I suggested the possible localization of Letm1 protein either to the chloroplast envelope membrane or the thylakoid membrane. If we assume Letm1 is localized in the thylakoid membrane that influxes calcium to the luminal side, disruption of this protein possibly leads to a deficiency in calcium concentration on the lumen side which in turn causes disruptions in several critical core proteins, such as PsbO from the oxygen-evolving complex (OEC) family of photosystem II. Our result in Fig. 27 A, B and C supports this hypothesis. Impaired influx activity of *letm1* mutant also possibly leads to overaccumulation of free calcium in the chloroplast envelope and consequently overaccumulation of calcium in cytosol since they cannot enter the chloroplast and as a result leads to higher accumulation of LHCSR3 (Fig 26A and B). In fact, higher accumulation of LHCSR3 is a side effect of *letm1* mutant. Indeed, main characteristic of *letm1* mutant refers to impairment to provide enough calcium in lumen side of thylakoid membrane which results in degradation of PSII reaction center and photobleaching. The author suggests that degradation of PSII core proteins due to deficiency of calcium overwhelms higher accumulation of LHCSR3 to protect photosystems, therefore overall, cells become highly photosensitive as in figure 27 clearly shown. It's worth reminding that I screened and isolated those mutants couldn't grow in calcium deficient medium. Therefore, lower calcium concentration in medium in case of *letm1* mutant resulted in lower accumulation of LHCSR3 (data are not shown) which in turn exaggerated the photosensitivity of mutant cells which led to strong photobleaching as I observed in *letm1* mutant in period of screening time. However, further experiments remain to be done to fully support our hypothesis.

The term CPLD originally came from Sabeeha S. Merchant et al., 2007 wherein they reported for the first-time sequencing of the ~120-megabase nuclear genome of *Chlamydomonas reinhardtii* and performed comparative phylogenomic analyses. They classified proteins in different categories and CPLD families refer to those expressed in chloroplast-containing cells and are conserved in the Plantae and diatoms. Furthermore, A phylogenetic tree file I made using IQ-Tree software shows *Chlamydomonas* homolog is grouped with various algae belonging to green, red, brown, and others. As far as I see from the attached NCBI Blast result tree, Cre12.g538700 is more closely related to algal genes than to land plants and animal homologs. This algal gene family is widely conserved in plastid-harboring species, which makes it tempt to speculate that this gene

might be associated with plastid functions (Fig 29). One transmembrane domain was detected using the TMHMM program (http://www.cbs.dtu.dk/services/TMHMM) and another SMART Domain search program (http://smart.embl-heidelberg.de) predicted a transmembrane domain (Fig 28).

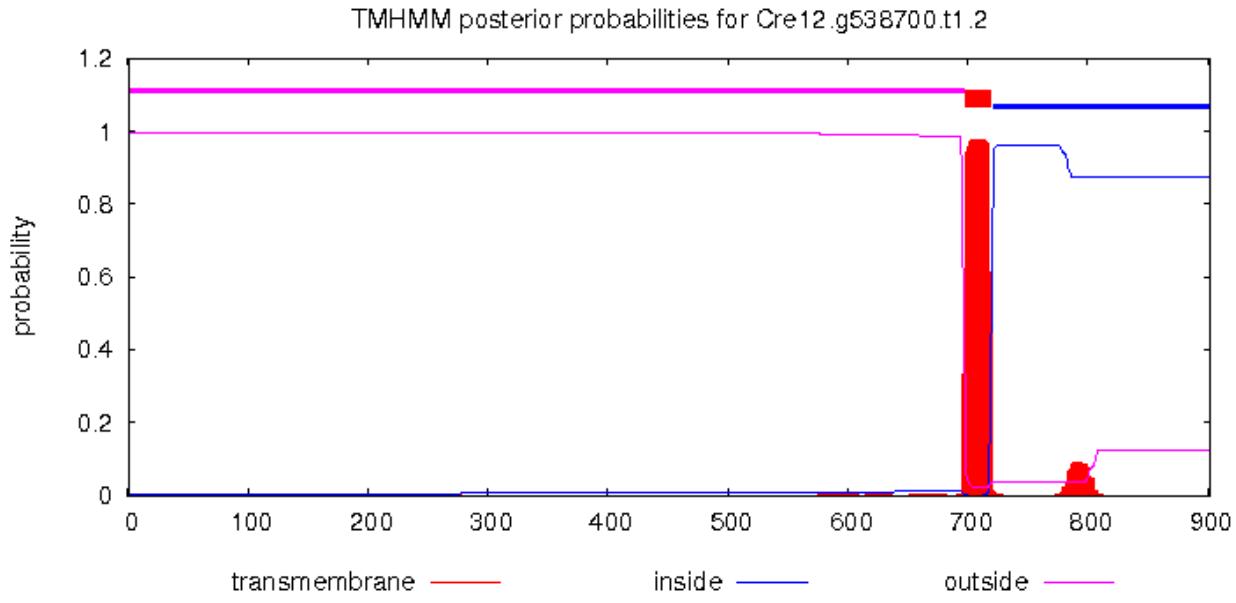

Fig 28 TMHMM program detected a transmembrane domain in LETM1 protein. The http://www.cbs.dtu.dk/services/TMHMM/TMHMM2.0b.guide.php server was applied by using TMHMM programs for prediction of transmembrane helices. The program takes proteins in FASTA format. The prediction gives the most probable location and orientation of transmembrane helices in the sequence. Red bars indicate transmembrane domains, blue lines indicate intracellular loops and magenta lines indicate extracellular loops. X axis shows number of amino acids and Y axis shows probability of prediction based on hidden markov model [HMM].

Thus, it is very likely Cre12.g538700 is a transmembrane protein. One the other hand Terashima et al., 2011 experimentally confirmed CPLD62 is a chloroplast-localized protein (Terashima et al., 2010).

Note: For referring to Terahsima et al paper, all the four proteins below are identical.

JGI.v5.5: Cre12.g538700.t1.2

jgi|Chlre3|147086|Chlre2_kg.scaffold_18000011

jgi|Chlre4|147086|Chlre2_kg.scaffold_18000011
NCBI Genbank: XP_001692965

LETM1-like proteins are known to be inner mitochondrial membrane proteins which play a role in potassium/calcium and hydrogen ion exchange. The *LETM1* gene was first reported in 1999 and is missing in patients suffer from Wolf-Hirschhorn Syndrome (WHS), which is a syndrome that includes severe mental and development retardation (Battaglia et al., 1999). In mammalian cells, LETM1 was hypothesized to potentially form a transporter via oligomerization (Jiang et al., 2013). Moreover, as determined using a genome-wide RNA interference (RNAi) screening method in *Drosophila* S2 cells, LETM1 may function as a Ca^{2+}/H^{+} antiporter. LETM1 can uptake Ca^{2+} across the mitochondrial inner membrane and can extrude H^{+} simultaneously when the concentration of cytosolic Ca^{2+} is lower than 1 μM (Jiang et al., 2009). However, the molecular mechanism of how LETM1 anti-transports Ca^{2+} and H^{+} still remains elusive.

Complementation of the mutant phenotype by *Letm1* gene

The plasmid carrying the LETM1 full cDNA is already constructed and sequencing analysis confirmed the constructed plasmid didn't have any point mutation, deletion or changes. I am in this step of analysis now and analysis needs to be processed to determine whether functional complementation can rescue *letm1* mutant phenotype.

LETM1 anti-transport Ca^{2+} and H^{+} in vitro

To investigate activity and confirm whether LETM1 forms a functional transporter, *Letm1* cDNA is in process to be expressed in *Escherichia coli* system and the purified recombinant protein will be analyzed through the cation including Ca^{2+} flux monitoring in presence of pH gradient by using patch clamp method.

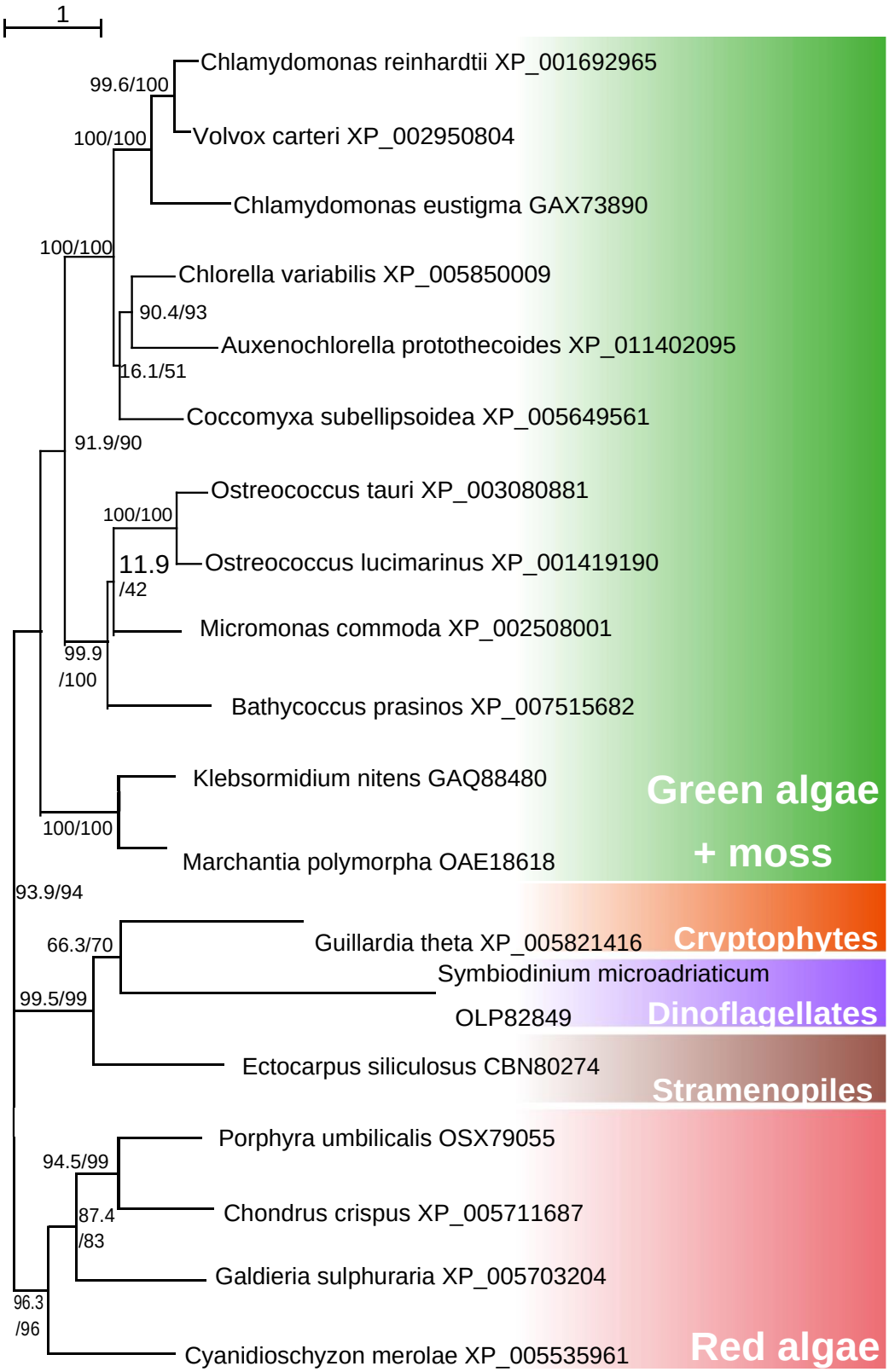
1
Chlamydomonas reinhardtii XP_001692965
99.6/100
Volvox carteri XP_002950804
100/100
Chlamydomonas eustigma GAX73890
100/100
Chlorella variabilis XP_005850009
90.4/93
Auxenochlorella protothecoides XP_011402095
16.1/51
Coccomyxa subellipsoidea XP_005649561
91.9/90
Ostreococcus tauri XP_003080881
100/100
11.9
/42
Ostreococcus lucimarinus XP_001419190
Micromonas commoda XP_002508001
99.9
/100
Bathycoccus prasinos XP_007515682
Klebsormidium nitens GAQ88480
100/100
Marchantia polymorpha OAE18618
Green algae
+ moss
93.9/94
66.3/70
Guillardia theta XP_005821416
Cryptophytes
Symbiodinium microadriaticum
99.5/99
OLP82849
Dinoflagellates
Ectocarpus siliculosus CBN80274
Stramenopiles
Porphyra umbilicalis OSX79055
94.5/99
87.4
/83
Chondrus crispus XP_005711687
Galdieria sulphuraria XP_005703204
96.3
/96
Cyanidioschyzon merolae XP_005535961
Red algae

Fig 29 Phylogenetic tree of Chlamydomonas LETM1 protein. The LETM-like gene sequences were conceptually translated into proteins and used for multiple sequence alignment and phylogenetic analysis using maximum likelihood tree. As it shown above, Chlamydomonas homolog is grouped with various algae belonging to green, red and brown algae and others. The results of bootstrap analyses using RAxML are shown on each branch.

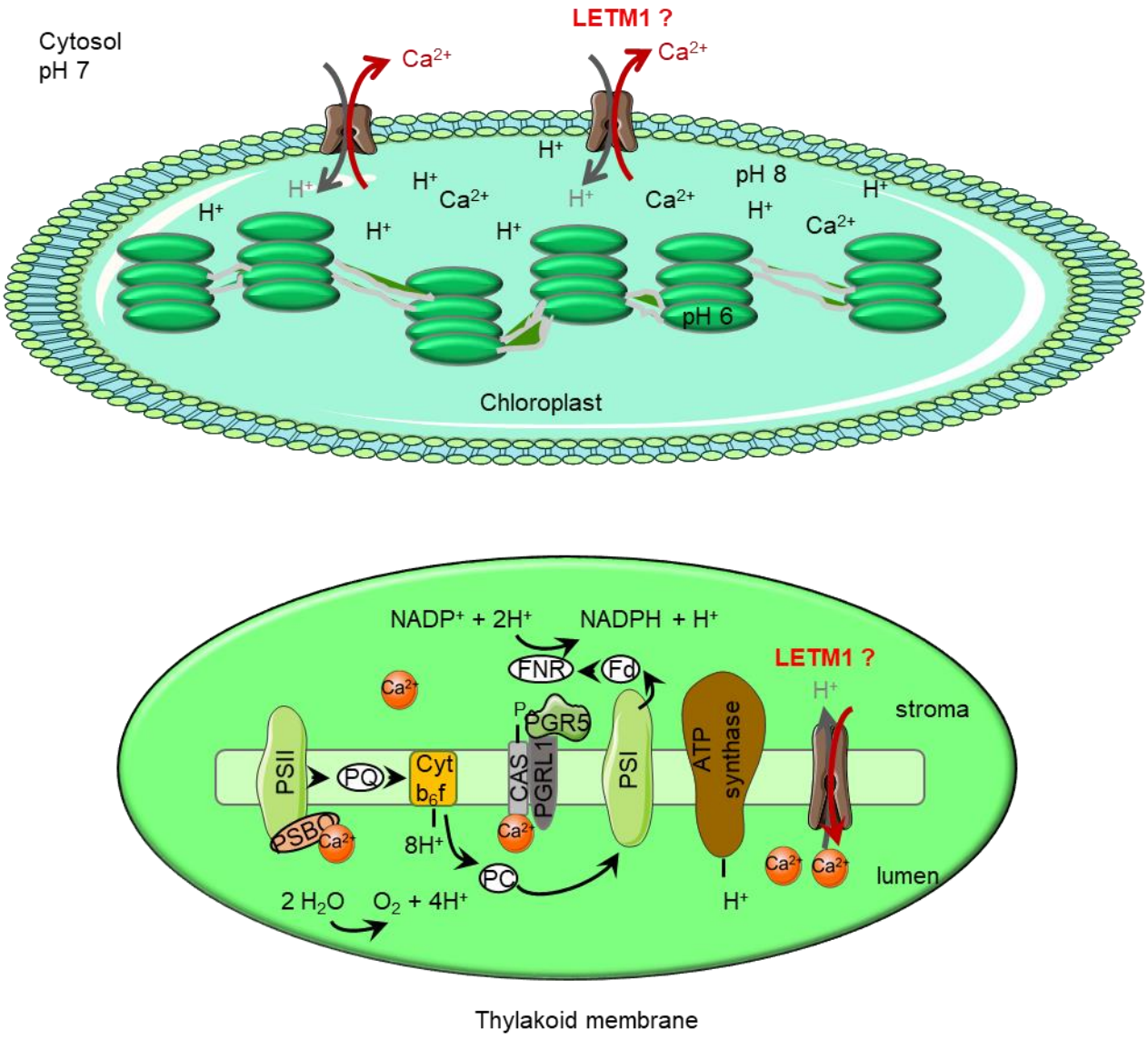

Fig 30 Dynamics of calcium signaling in chloroplast stroma (A) or thylakoid lumen (B) with hypothetical localization of LETM1. In this model LETM1 is a candidate anti-transporter

calcium channel which can be either localized in chloroplast envelope membrane or across thylakoide membrane. If LETM1 placed across thylakoid membrane, it can influx Ca^{2+} to thylakoid luminal pool which is essential for important photosystem II core proteins as well as CAS. The impact of calcium is illustrated by orange-colored Ca^{2+} ions. This model is constructed based on information from Hochmal et al 2015 (Hochmal et al., 2015).

Chapter 6

General discussion

This project not only familiarized me with the contribution of the circadian clock to the mechanisms of photoacclimation that assist microalgae in not only synchronizing with environmental changes but also assist in determining the magnitude of response to better harness resources, energy, and feedback mechanisms to ensure survival and enhance the fitness of the individual. I was interested to find out that LHCSR3 gene expression follows rhythmicity as shown in Fig 8 and 25. Furthermore, the project gave me a priceless understanding of the role of photoreceptors and light quality in photoprotection. My findings regarding the involvement of a circadian component into the photoprotection mechanisms provides a new viewpoint for thinking about the adaptive significance of the circadian clock. By my knowledge our project could present the first evidence of involvement of circadian components in photoprotection in *C. reinhardtii*. During the project I mainly focused on characterization of ROC75 which is one the central elements of the circadian clock in *Chlamydomonas reinhardtii*. I analyzed the possible role of ROC proteins on photoacclimation, particularly LHCSR3 regulation. I showed ROC75 acts as an attenuator for the circadian clock to control *LHCSR3* expression with blue and red light as stimuli. ROC75 has GARP DNA-binding motifs similar to that of *A. thaliana* LUX ARRHYTHMO (LUX) (also termed PHYTOCLOCK 1 (PCL1)). My findings on the photoprotective role of ROC75 may bring a new viewpoint for plant researchers to investigate the role of the circadian clock on photoprotection. It is worth mentioning here that I modified the dark/light cycle entrainment of cells which is commonly used by dividing the 12 h light into three sections (3:6:3 h red:red+green+blue:red respectively) to more closely mimic the spectral fingerprint of natural light at dawn, noon and dusk.

Working on this project, including the laboratory techniques I used, was a good foundation for my second project on phototropin dependent calcium signaling, as well as my third project designing and developing a robust and reliable high throughput screening method to identify mutants using forward genetics as fully described in chapter 3. My findings not only imply that cytosolic Ca^{2+} is the key factor for the integrated signal between PHOT and ETR pathways but also sheds more light on these pathways involvement in the regulation of LHCSR3 and photoprotection.

Our results in Fig 13 show both basal level of cytosolic Ca^{2+} treated with 1-hour illumination with blue light or Ca^{2+} imaging traces of cells exposed to acute stimulation with blue light were elevated

only in wild type cells but not the *phot* mutant. Thus, we can conclude that blue light-dependent Ca^{2+} signaling is dependent on phototropin.

Our results show that blue light can stimulate IP_3 production in WT cells, however in the *phot* mutant IP_3 accumulation under blue light was not observed suggesting that phototropin regulates PLC-catalyzed IP_3 formation.

In order to achieve more direct evidence that accumulation of IP_3 is a major regulator of LHCSR3 expression, depleting the free IP_3 concentration using either an IP_3 sponge (a high-affinity fragment of the mammalian IP_3-binding site from IP_3R) or by expressing IP_3 3-kinase to phosphorylate IP_3 to IP_4 (Dewaste et al., 2002) will be undertaken in future experiments. I could find the homologue of mammalian IP_3 3-K in *Chlamydomonas reinhardtii* at phytozome ver. 12 named as IPK Cre12.g555450. Both mammalian and *Chlamydomonas* IP_3 3-K have inositol polyphosphate kinase domain in their protein structure. These ideas will be assessed in future experiments.

We also found cAMP-dependent induction of LHCSR3 expression involves intracellular Ca^{2+} signaling.

Petrotsus et al. (2016) found a link between PHOT-dependent Ca^{2+} signaling and cAMP, that we were able to reproduce. Both IP_3 and diacylglycerol, products of PLC activation, affect cAMP formation. Ca^{2+} mobilized from intracellular stores by IP_3 forms a complex with CaM and the Ca^{2+}-CaM complex can directly bind to certain forms of adenylyl cyclases to activate them. On the other hand, there are also several reports that show that the hydrolysis of PIP2 is regulated by cAMP and cAMP-dependent protein kinase A (PKA). Therefore, we can easily imagine crosstalk between PKA and PLC signaling pathways ultimately leading to intracellular Ca^{2+} increase and LHCSR3 expression. Further analysis will be necessary to characterize the exact functions of cAMP PHOT-dependent Ca^{2+} signaling.

So far we don't have any strong data to support whether the IP_3R on the ER membrane is involved in the regulation of intracellular Ca^{2+} signaling. *ip3r* mutants we used to be generated by insertional mutagenesis as shown in Fig 20 exhibited 40% drops in accumulation of LHCSR3 as well as qE value however this reduction was not as strong as we expected. If we investigate the role and function of IP_3R in mammalian cells, cytosolic calcium level is not only regulated by IP_3R but also by other channels. Wu et al, showed Trpp channel 15 interact with IP_3R to regulate ER stress

calcium release (Wu et al., 2018). The similar scenario can be fit with cytosolic calcium regulation in *Chlamydomonas reinhardtii*. This hypothesis is under investigation and experiments with several *Chlamydomonas* Trpp channel candidates are in process.

Taken all together, these results support the idea of two different signaling pathways sharing a common mediator, Ca^{2+} signaling, and regulating *LHCSR3* expression. I further suggest, in the presence of blue light, the photosynthesis activity (ETR) leads to an efflux of calcium from chloroplast to cytosol. This Ca^{2+} efflux raises the $[Ca^{2+}]_{cyt}$ from a minimal to a higher level (Fig 31) which is sufficient to activate IP_3R in the presence of IP_3. Once the IP_3R is activated, a further increase in $[Ca^{2+}]_{cyt}$ is achieved upon Ca^{2+} release from the ER, promoting LHCSR3 protein expression. If this hypothesis is true, blocking the ETR pathway by DCMU should inhibit the Ca^{2+} efflux from chloroplast and maintain a low level of $[Ca^{2+}]_{cyt}$. Indeed, others and I have shown that DCMU blockade of ETR strongly repressed LHCSR3 protein and mRNA levels as well as qE induction.

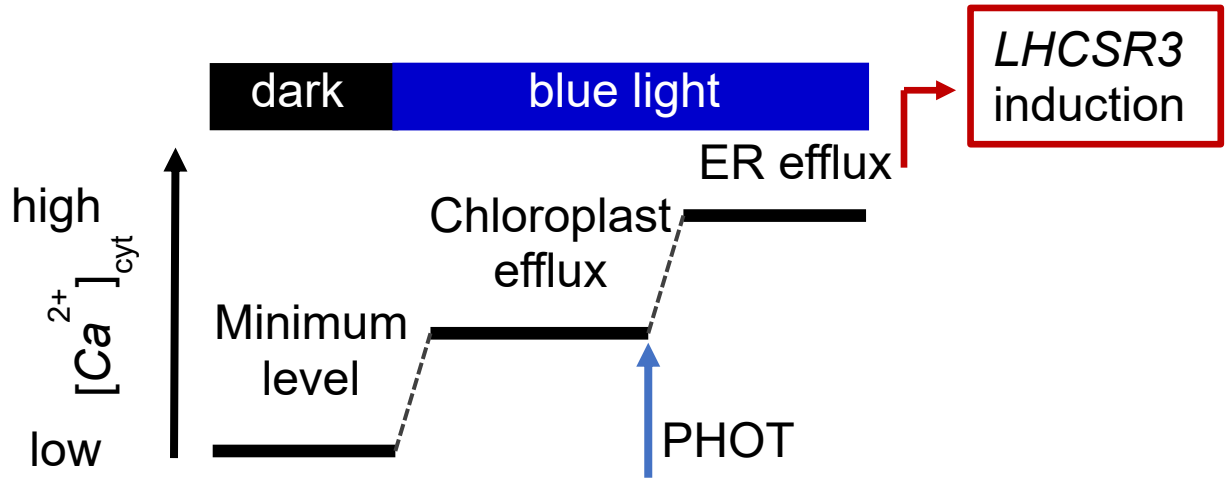

Fig 31 Diagrammatic scheme of the effect of blue light on cytosolic calcium concentration through organellar diffusion. In this three-step hypothesis, blue or red-light triggers calcium efflux from the chloroplast which consequently, only in presence of phototropin mediated IP_3 formation, stimulates ER to release high concentrations of calcium into the cytosol.

In my third project I established a high-throughput forward genetics approach to screen LHCSR3 related mutants _via_ bioluminescence derived from a luciferase reporter gene under varying light cues. I screened more than 7000 transformants to isolate mutants, however, scaling up a

screening of a larger number of transformants (~20,000) will increase the possibility of revealing unpredicted gene(s) which may be involved in calcium signaling mediated LHCSR3 regulation. On the other hand, since cytosolic calcium signaling processes are a fast physiological response, my reporter strain can monitor both transcriptional and translational behavior of the LHCSR3 endogenous gene and is potentially a very powerful tool.

However, I assume *Chlamydomonas* LETM1 has function similar to PPF1 in plant which is a H^+/Ca^{2+} antiport across the thylakoid membrane. Overexpression and knockdown of the thylakoid protein Post-Floral-specific gene 1 (PPF1) led to an increased and decreased calcium storage capacity of *Arabidopsis* guard cells, respectively. Further research on *letm1* should yield important information on calcium dependent regulation of *LHCSR3* and with the expanded view it will shed light on the regulation of photosynthetic electron flow by the interplay of Ca^{2+}.

References

Aro, E.-M., Virgin, I., and Andersson, B. (1993) Photoinhibition of Photosystem II. Inactivation, protein damage and turnover. *Biochim Biophys Acta - Bioenerg*. 1143: 113–134.

Battaglia, A., Carey, J.C., Cederholm, P., Viskochil, D.H., Brothman, A.R., and Galasso, C. (1999) Natural history of Wolf-Hirschhorn syndrome: experience with 15 cases. *Pediatrics*. 103: 830–6.

Baum, G., Long, J.C., Jenkins, G.I., and Trewavas, A.J. (1999) Stimulation of the blue light phototropic receptor NPH1 causes a transient increase in cytosolic Ca²⁺ *Proc Natl Acad Sci*. 96: 13554 -13559.

Berthold, P., Schmitt, R., and Mages, W. (2002) An engineered Streptomyces hygroscopicus aph 7" gene mediates dominant resistance against hygromycin B in Chlamydomonas reinhardtii. *Protist*. 153: 401–412.

Björkman, O., and Demmig, B. (1987) Photon yield of O2 evolution and chlorophyll fluorescence characteristics at 77 K among vascular plants of diverse origins. *Planta*. 170: 489–504.

Bothwell, J.H.F., Brownlee, C., Hetherington, A.M., Ng, C.K.-Y., Wheeler, G.L., and McAinsh, M.R. (2006) Biolistic delivery of Ca2+ dyes into plant and algal cells. *Plant J*. 46: 327–35.

Boyce, M., and Yuan, J. (2006) Cellular response to endoplasmic reticulum stress: a matter of life or death. *Cell Death Differ*. 13: 363.

Chihiro, H., and Katsuhiko, M. (2017) IP3 receptor mutations and brain diseases in human and rodents. *J Neurochem*. 141: 790–807.

Cole, D.G. (2003) The intraflagellar transport machinery of Chlamydomonas reinhardtii. *Traffic*. 4: 435–442.

Collingridge, P.W., Wheeler, G., and Brownlee, C. (2012) The molecular mechanisms of calcium signalling in Chlamydomonas flagella. *Cilia*. 1: P19.

Dewaste, V., Roymans, D., Moreau, C., and Erneux, C. (2002) Cloning and expression of a full-

length cDNA encoding human inositol 1,4,5-trisphosphate 3-kinase B. *Biochem Biophys Res Commun*. 291: 400–5.

Edel, K.H., and Kudla, J. (2015) Increasing complexity and versatility: how the calcium signaling toolkit was shaped during plant land colonization. *Cell Calcium*. 57: 231–46.

Ehlers, C., Frank, E., and DJ, K. (1988) Social zeitgebers and biological rhythms: A unified approach to understanding the etiology of depression. *Arch Gen Psychiatry*. 45: 948–952.

Erickson, E., Wakao, S., and Niyogi, K.K. (2015) Light stress and photoprotection in Chlamydomonas reinhardtii. *Plant J*. 82: 449–465.

Gafni, J., Munsch, J.A., Lam, T.H., Catlin, M.C., Costa, L.G., Molinski, T.F., et al. (1997) Xestospongins: potent membrane permeable blockers of the inositol 1,4,5-trisphosphate receptor. *Neuron*. 19: 723–33.

Garbison, K.E., Heinz, B.A., and Lajiness, M.E. (2004) IP-3/IP-1 Assays, Assay Guidance Manual.

González-Ballester, D., de Montaigu, A., Galván, A., and Fernández, E. (2005) Restriction enzyme site-directed amplification PCR: a tool to identify regions flanking a marker DNA. *Anal Biochem*. 340: 330–335.

Gorman, D.S., and Levine, R.P. (1965) Cytochrome f and plastocyanin: their sequence in the photosynthetic electron transport chain of Chlamydomonas reinhardi. *Proc Natl Acad Sci*. 54: 1665–1669.

Harada, A., and Shimazaki, K. (2007) Phototropins and Blue Light-dependent Calcium Signaling in Higher Plants†. *Photochem Photobiol*. 83: 102–111.

Harris, E.H. (2001) Chlamydomonas as amodel organism. *Annu Rev Plant Physiol Plant Mol Biol*. 52: 363–406.

Hochmal, A.K. arin., Schulze, S., Trompelt, K., and Hippler, M. (2015) Calcium-dependent regulation of photosynthesis. *Biochim Biophys Acta*. 1847: 993–1003.

Horton, P., Ruban, A. V., and Walters, R.G. (1996) Regulation of light harvesting in green plants. *Annu Rev Plant Physiol Plant Mol Biol*. 47: 655–684.

Jiang, D., Zhao, L., and Clapham, D.E. (2009) Genome-wide RNAi screen identifies Letm1 as a mitochondrial Ca2+/H+ antiporter. *Science*. 326: 144–7.

Jiang, D., Zhao, L., Clish, C.B., and Clapham, D.E. (2013) Letm1, the mitochondrial Ca2+/H+ antiporter, is essential for normal glucose metabolism and alters brain function in Wolf-Hirschhorn syndrome. *Proc Natl Acad Sci U S A*. 110: 2249-2254.

Keller, L.C., Romijn, E.P., Zamora, I., Yates, J.R., and Marshall, W.F. (2005) Proteomic analysis of isolated chlamydomonas centrioles reveals orthologs of ciliary-disease genes. *Curr Biol*. 15: 1090–8.

Kim, H.Y., Coté, G.G., and Crain, R.C. (1996) Inositol 1,4,5-trisphosphate may mediate closure of K^+ channels by light and darkness in Samanea saman motor cells. *Planta*. 198: 279–287.

Knight, H. (2000) Calcium signaling during abiotic stress in plants. *Int. Rev. Cytol.* 192: 269–324.

Krogh, A., Larsson, B., Heijne, G. and Sonnhammer, E. L. (2001) Predicting transmembrane protein topology with a hidden Markov model: application to complete genomes. *J. Mol. Biol.* 305: 567–580.

Kuin, H., Koerten, H., Ghijsen, W.E., Munnik, T., van den Ende, H., and Musgrave, A. (2000) Chlamydomonas contains calcium stores that are mobilized when phospholipase C is activated. *Planta*. 210: 286–94.

Li, X., Zhang, R., Patena, W., Gang, S.S., Blum, S.R., Ivanova, N., et al. (2016) An indexed, mapped mutant library enables reverse genetics studies of biological processes in Chlamydomonas reinhardtii. *Plant Cell*. 28: 367 LP-387.

Lu, Y.-T., Hidaka, H., and Feldman, L.J. (1996) Characterization of a calcium/calmodulin-dependent protein kinase homolog from maize roots showing light-regulated gravitropism. *Planta*. 199: 18–24.

Maruyama, S., Tokutsu, R., and Minagawa, J. (2014) Transcriptional regulation of the stress-responsive light harvesting complex genes in Chlamydomonas reinhardtii. *Plant Cell Physiol*. 55: 1304–1310.

Matsuo, T., and Ishiura, M. (2011) Chlamydomonas reinhardtii as a new model system for studying the molecular basis of the circadian clock. *FEBS Lett*. 585: 1495–1502.

Matsuo, T., Okamoto, K., Onai, K., Niwa, Y., Shimogawara, K., and Ishiura, M. (2008) A systematic forward genetic analysis identified components of the Chlamydomonas circadian system. *Genes Dev*. 22: 918–930.

McAinsh, M.R., and Pittman, J.K. (2009) Shaping the calcium signature. *New Phytol*. 181: 275–94.

McClung, C.R. (2006) Plant Circadian Rhythms. *Plant Cell Online*. 18: 792–803.

Merchant, S.S., Prochnik, S.E., Vallon, O., Harris, E.H., Karpowicz, J., Witman, G.B., et al. (2007) The Chlamydomonas genome reveals the evolution of key animal and plant functions. *Science* 318: 245–250.

Millar, A.J. (2003) A suite of photoreceptors entrains the plant circadian clock. *J Biol Rhythms*. 18: 217–26.

Minagawa, J. (2011) State transitions--the molecular remodeling of photosynthetic supercomplexes that controls energy flow in the chloroplast. *Biochim Biophys Acta*. 1807: 897–905.

Motiwalla, M.J., Sequeira, M.P., and D'Souza, J.S. (2014) Two calcium-dependent protein kinases from Chlamydomonas reinhardtii are transcriptionally regulated by nutrient starvation. *Plant Signal Behav*. 9: e27969.

Müller, N., Wenzel, S., Zou, Y., Künzel, S., Sasso, S., Weiß, D., et al. (2017) A Plant Cryptochrome Controls Key Features of the Chlamydomonas Circadian Clock and its Life Cycle. *Plant Physiol*.

Muller, P. (2001) Non-Photochemical Quenching. A Response to Excess Light Energy. *Plant Physiol*. 125: 1558–1566.

Munnik, T., Irvine, R.F., and Musgrave, A. (1998) Phospholipid signalling in plants. *Biochim Biophys Acta*. 1389: 222–72.

Nilkens, M., Kress, E., Lambrev, P., Miloslavina, Y., Müller, M., Holzwarth, A.R., et al. (2010)

Identification of a slowly inducible zeaxanthin-dependent component of non-photochemical quenching of chlorophyll fluorescence generated under steady-state conditions in Arabidopsis. *Biochim Biophys Acta*. 1797: 466–75.

Nishio, J.N., Sun, J. and Vogelmann, T.C. (1993) Carbon fixation gradients across spinach leaves do not follow internal light gradients. *Plant Cell 5:* 953-961.

Niwa, Y., Matsuo, T., Onai, K., Kato, D., Tachikawa, M., and Ishiura, M. (2013) Phase-resetting mechanism of the circadian clock in Chlamydomonas reinhardtii. *Proc Natl Acad Sci*. 110: 13666–13671.

Niyogi, K.K. (1999) Photoprotection revisited: Genetic and Molecular Approaches. *Annu Rev Plant Physiol Plant Mol Biol*. 50: 333–359.

Niyogi, K.K., Bjorkman, O., and Grossman, A.R. (1997) Chlamydomonas Xanthophyll Cycle Mutants Identified by Video Imaging of Chlorophyll Fluorescence Quenching. *Plant Cell*. 9: 1369-1380.

Ohnishi, N., Allakhverdiev, S.I., Takahashi, S., Higashi, S., Watanabe, M., Nishiyama, Y., et al. (2005) Two-Step Mechanism of Photodamage to Photosystem II: Step 1 Occurs at the Oxygen-Evolving Complex and Step 2 Occurs at the Photochemical Reaction Center. *Biochemistry*. 44: 8494–8499.

Peers, G., Truong, T.B., Ostendorf, E., Busch, A., Elrad, D., Grossman, A.R., et al. (2009) An ancient light-harvesting protein is critical for the regulation of algal photosynthesis. *Nature*. 462: 518–521.

Petroutsos, D., Busch, A., Janßen, I., Trompelt, K., Bergner, S.V., Weinl, S., et al. (2011) The Chloroplast Calcium Sensor CAS Is Required for Photoacclimation in *Chlamydomonas reinhardtii*. *Plant Cell*. 23: 2950–2963.

Petroutsos, D., Tokutsu, R., Maruyama, S., Flori, S., Greiner, A., Magneschi, L., et al. (2016) A blue-light photoreceptor mediates the feedback regulation of photosynthesis. *Nature*. 537: 563–566.

Portis, A.R., and Heldt, H.W. (1976) Light-dependent changes of the Mg2+ concentration in the stroma in relation to the Mg2+ dependency of CO2 fixation in intact chloroplasts. *Biochim*

Biophys Acta. 449: 434–6.

Quarmby, L.M., and Hartzell, H.C. (1994) Two distinct, calcium-mediated, signal transduction pathways can trigger deflagellation in Chlamydomonas reinhardtii. *J Cell Biol*. 124: 807–15.

Quarmby, L.M., Yueh, Y.G., Cheshire, J.L., Keller, L.R., Snell, W.J., and Crain, R.C. (1992) Inositol phospholipid metabolism may trigger flagellar excision in Chlamydomonas reinhardtii. *J Cell Biol*. 116: 737–44.

Sanchez, A., Shin, J., and Davis, S.J. (2011) Abiotic stress and the plant circadian clock. *Plant Signal Behav*. 6: 223–231.

Sharma, V.K. (2003) Adaptive significance of circadian clocks. *Chronobiol Int*. 20: 901–19.

Shimogawara, K., Fujiwara, S., Grossman, A., and Usuda, H. (1998) High-efficiency transformation of Chlamydomonas reinhardtii by electroporation. *Genetics*. 148: 1821–8.

Somersalo, S., and Krause, G.H. (1989) Photoinhibition at chilling temperature. *Planta*. 177: 409–416.

Stangherlin, A., and Reddy, A.B. (2013) Regulation of circadian clocks by redox homeostasis. *J Biol Chem*. 288: 26505–26511.

Sueoka, N. (1960) Mitotic Replication of Deoxyribonucleic Acid in Chlamydomonas Reinhardi. *Proc Natl Acad Sci U S A*. 46: 83–91.

Sumi, M., Kiuchi, K., Ishikawa, T., Ishii, A., Hagiwara, M., Nagatsu, T., et al. (1991) The newly synthesized selective Ca2+/calmodulin dependent protein kinase II inhibitor KN-93 reduces dopamine contents in PC12h cells. *Biochem Biophys Res Commun*. 181: 968–75.

Takahashi, H., Iwai, M., Takahashi, Y., and Minagawa, J. (2006) Identification of the mobile light-harvesting complex II polypeptides for state transitions in Chlamydomonas reinhardtii *Proc Natl Acad Sci U S A*. 103: 477-482.

Tam, L.W., and Lefebvre, P.A. (1993) Cloning of flagellar genes in Chlamydomonas reinhardtii by DNA insertional mutagenesis. *Genetics*. 135: 375-384.

Taylor, C.W., and Tovey, S.C. (2010) IP(3) receptors: toward understanding their activation.

Cold Spring Harb Perspect Biol. 2: a004010.

Terashima, M., Specht, M., Naumann, B., and Hippler, M. (2010) Characterizing the anaerobic response of Chlamydomonas reinhardtii by quantitative proteomics. *Mol Cell Proteomics*. 9: 1514–32.

Vallone, D., Gondi, S.B., Whitmore, D., and Foulkes, N.S. (2004) E-box function in a period gene repressed by light. *Proc Natl Acad Sci*. 101: 4106 - 4111.

Weinl, S., Held, K., Schlücking, K., Steinhorst, L., Kuhlgert, S., Hippler, M., et al. (2008) A plastid protein crucial for Ca2+-regulated stomatal responses. *New Phytol*. 179: 675–86.

Weiss, B., and Hait, W.N. (1977) Selective cyclic nucleotide phosphodiesterase inhibitors as potential therapeutic agents. *Annu Rev Pharmacol Toxicol*. 17: 441–77.

Wheeler, G.L., and Brownlee, C. (2008) Ca2+ signalling in plants and green algae--changing channels. *Trends Plant Sci*. 13: 506–14.

White, P.J., and Broadley, M.R. (2003) Calcium in plants. *Ann Bot*. 92: 487–511.

Wu, Q., Gao, K., Zheng, S., Zhu, X., Liang, Y., and Pan, J. (2018) Calmodulin regulates a TRP channel (ADF1) and phospholipase C (PLC) to mediate elevation of cytosolic calcium during acidic stress that induces deflagellation in Chlamydomonas. *FASEB J*. 32: 3689–3699.

Yamano, T., Miura, K., and Fukuzawa, H. (2008) Expression Analysis of Genes Associated with the Induction of the Carbon-Concentrating Mechanism in Chlamydomonas reinhardtii *Plant Physiol*. 147: 340 LP-354.

Yerushalmi, S., and Green, R.M. (2009) Evidence for the adaptive significance of circadian rhythms. *Ecol Lett*. 12: 970–981.

Yoon, H.S., Hackett, J.D., Ciniglia, C., Pinto, G., and Bhattacharya, D. (2004) A molecular timeline for the origin of photosynthetic eukaryotes. *Mol Biol Evol*. 21: 809–18.

Zavafer, A., Cheah, M.H., Hillier, W., Chow, W.S., and Takahashi, S. (2015) Photodamage to the oxygen evolving complex of photosystem II by visible light. *Sci Rep*. 5: 1–8.

Zorin, B., Lu, Y., Sizova, I., and Hegemann, P. (2009) Nuclear gene targeting in Chlamydomonas as exemplified by disruption of the PHOT gene. *Gene*. 432: 91–96.